

Deep Face Recognition: A Survey

Mei Wang, Weihong Deng

School of Information and Communication Engineering,
Beijing University of Posts and Telecommunications, Beijing, China.

wm0245@126.com, whdeng@bupt.edu.cn

Abstract—Deep learning applies multiple processing layers to learn representations of data with multiple levels of feature extraction. This emerging technique has reshaped the research landscape of face recognition since 2014, launched by the breakthroughs of DeepFace and DeepID methods. Since then, deep face recognition (FR) technique, which leverages the hierarchical architecture to learn discriminative face representation, has dramatically improved the state-of-the-art performance and fostered numerous successful real-world applications. In this paper, we provide a comprehensive survey of the recent developments on deep FR, covering the broad topics on algorithms, data, and scenes. First, we summarize different network architectures and loss functions proposed in the rapid evolution of the deep FR methods. Second, the related face processing methods are categorized into two classes: “one-to-many augmentation” and “many-to-one normalization”. Then, we summarize and compare the commonly used databases for both model training and evaluation. Third, we review miscellaneous scenes in deep FR, such as cross-factor, heterogeneous, multiple-media and industry scenes. Finally, potential deficiencies of the current methods and several future directions are highlighted.

I. INTRODUCTION

Due to its nonintrusive and natural characteristics, face recognition (FR) has been the prominent biometric technique for identity authentication and has been widely used in many areas, such as military, finance, public security and daily life. FR has been a long-standing research topic in the CVPR community. In the early 1990s, the study of FR became popular following the introduction of the historical Eigenface approach [164]. The milestones of feature-based FR over the past years are presented in Fig. 1, in which the times of four major technical streams are highlighted. The holistic approaches derive the low-dimensional representation through certain distribution assumptions, such as linear subspace [13][118][44], manifold [70][199][43], and sparse representation [184][221][40][42]. This idea dominated the FR community in the 1990s and 2000s. However, a well-known problem is that these theoretically plausible holistic methods fail to address the uncontrolled facial changes that deviate from their prior assumptions. In the early 2000s, this problem gave rise to local-feature-based FR. Gabor [104] and LBP [5], as well as their multilevel and high-dimensional extensions [222][26][41], achieved robust performance through some invariant properties of local filtering. Unfortunately, handcrafted features suffered from a lack of distinctiveness and compactness. In the early 2010s, learning-based local descriptors were introduced to the FR community [21][95][22], in which local filters are learned for better distinctiveness, and the encoding codebook is learned for better compactness. However, these shallow representations

still have an inevitable limitation on robustness against the complex nonlinear facial appearance variations.

In general, traditional methods attempted to solve FR problem by one or two layer representation, such as filtering responses or histogram of the feature codes. The research community studied intensively to separately improve the preprocessing, local descriptors, and feature transformation, which improve face recognition accuracy slowly. By the continuous improvement of a decade, “shallow” methods only improve the accuracy of the LFW benchmark to about 95% [26], which indicates that “shallow” methods are insufficient to extract stable identity feature against unconstrained facial variations. Due to the technical insufficiency, facial recognition systems were often reported with unstable performance or failures with countless false alarms in real-world applications.

But all that changed in 2012 when AlexNet won the ImageNet competition by a large margin using a technique called deep learning [94]. Deep learning methods, such as convolutional neural networks, use a cascade of multiple layers of processing units for feature extraction and transformation. They learn multiple levels of representations that correspond to different levels of abstraction. The levels form a hierarchy of concepts, showing strong invariance to the face pose, lighting, and expression changes, as shown in Fig. 2. It can be seen from the figure that the first layer of the deep neural network is somewhat similar to the Gabor feature found by human scientists with years of experience. The second layer learned more complex texture features. The features of the third layer are more complex, and some simple structures have begun to appear, such as high-bridged nose and big eyes. In the fourth, the network output is enough to explain a certain facial attribute, which can make a special response to some clear abstract concepts such as smile, roar, and even blue eye. Deep CNN, the initial layers automatically learn the features designed for years or even decades, such as Gabor, SIFT (such as initial layers in Fig. 2), and the later layers further learn higher level abstraction. Finally, the combination of these higher level abstraction represents facial identity with unprecedented stability.

In 2014, DeepFace [160] achieved the state-of-the-art accuracy on the famous LFW benchmark [77], approaching human performance on the unconstrained condition for the first time (DeepFace: 97.35% vs. Human: 97.53%). Since then, research focus has shifted to deep-learning-based approaches, and the accuracy was dramatically boosted to above 99.80% in just three years. Deep learning technique has reshaped the research landscape of face recognition in almost all aspects such as algorithms, data sets, and even the evaluation protocols.

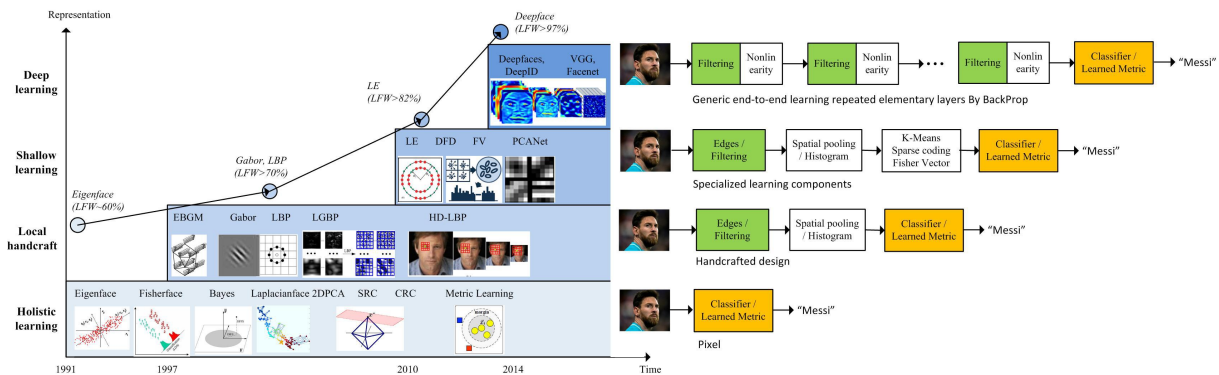


Fig. 1. Milestones of feature representation for FR. The holistic approaches dominated the FR community in the 1990s and 2000s. In the early 2000s and 2010s, Local-feature-based FR and learning-based local descriptors were introduced successively. In 2014, DeepFace [160] and DeepID [152] achieved state-of-the-art accuracy, and research focus has shifted to deep-learning-based approaches. As the representation pipeline becomes deeper and deeper, the LFW (Labeled Face in-the-Wild) performance steadily improves from around 60% to above 90%, while deep learning boosts the performance to 99.80% in only three years.

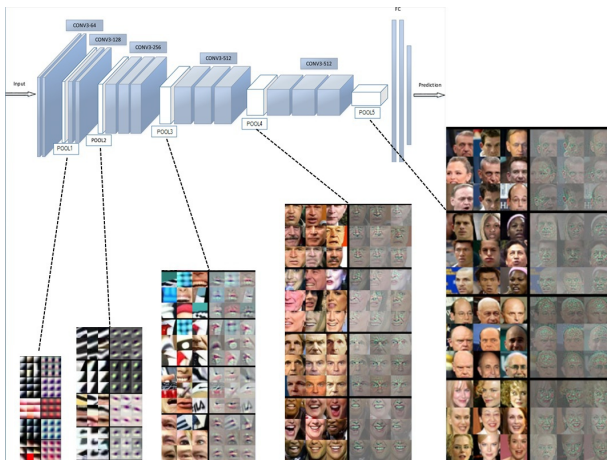


Fig. 2. The hierarchical architecture of deep FR. Algorithms consist of multiple layers of simulated neurons that convolute and pool input, during which the receptive-field size of simulated neurons are continually enlarged to integrate the low-level primary elements into multifarious facial attributes, finally feeding the data forward to one or more fully connected layer at the top of the network. The output is a compressed feature vector that represent the face. Such deep representation is widely considered the state-of-the-art technique for face recognition.

Therefore, it is of great significance to review the breakthrough and rapid development process in recent years. Although there have been several surveys on FR [231], [18], [3], [81], [143] and its subdomains, including illumination-invariant FR [247], 3D FR [143], pose-invariant FR [225], none of them aims to cover the methodologies on deep FR. In this survey, we focus on up-to-date deep-feature-learning-based FR, as well as its closely related database development, face processing, and face matching methods. Face detection and alignment are beyond our consideration, and one can refer to Ranjan et al. [130], who provided a brief review of a full deep FR pipeline. Specifically, the major contributions of this survey are as follows:

- A systematic review on the evolution of the network architectures and loss functions for deep FR. Various loss functions are studied and categorized into Euclidean-

distance-based loss, angular/cosine-margin-based loss and softmax loss and its variations. Both the mainstream network architectures, such as Deepface [160], DeepID series [156], [185], [152], [153], VGGFace [123], FaceNet [144], and VGGFace2 [20], and other specific architectures designed for FR are covered.

- We categorize the face processing methods, such as those used to handle recognition difficulty on pose change, into two classes: “one-to-many augmentation” and “many-to-one normalization”, and discuss how emerging generative adversarial network (GAN) [53] facilitate deep FR.
- A comparison and analysis on public available large-scale training data sets that are at vital importance for deep FR. Major FR benchmarks, such as LFW [77], IJB-A/B/C [93], [182], Megaface [89], and MS-Celeb-1M [59]. They are reviewed and compared, in term of the four aspects: training methodology, evaluation tasks and metrics, and recognition scenes, which provide an useful references for training and testing deep FR.
- Besides the common tasks defined by the mainstreaming databases, we summarize a dozen specific FR scenes that are still challenging for deep learning, such as anti-spoofing, cross-pose FR, and cross-age FR. By reviewing specially designed methods for these unsolved problems, we attempt to reveal the important issues for future research on deep FR.

The remainder of this survey is structured as follows. In Section II, we introduce some background concepts and terminology, and then we briefly introduce each component of FR. In Section III, different network architectures and loss functions are presented. Then, we summarize the algorithms for face processing and the datasets. In Section V, we briefly introduce several methods for deep FR with different scenes. Finally, the conclusion of this paper and discussion of future works are presented in Section VI.

II. OVERVIEW

A. Background Concepts and Terminology

As mentioned in [130], there are three modules needed for the whole system, as shown in Fig. 3. First, a face detector is used to localize faces in images or videos. Second, with the facial landmark detector, the faces are aligned to normalized canonical coordinates. Third, the FR module is implemented with these aligned face images. We only focus on the FR module throughout the remainder of this paper.

Furthermore, FR can be categorized as face verification and face identification. In either scenario, a set of known subjects is initially enrolled in the system (the gallery), and during testing, a new subject (the probe) is presented. Face verification computes one-to-one similarity between the gallery and probe to determine whether the two images are of the same subject, whereas face identification computes one-to-many similarity to determine the specific identity of a probe face. When the probe appears in the gallery identities, this is referred to as closed-set identification; when the probes include those who are not in the gallery, this is open-set identification.

B. Components of Face Recognition

Before a face image is fed to an FR module, face anti-spoofing, which recognizes whether the face is live or spoofed, can avoid different types of attacks. We treat it as one of the FR scenes and present it in Section VI-D3. Then, recognition can be performed. As shown in Fig. 3(c), an FR module consists of face processing, deep feature extraction and face matching, and it can be described as follows:

$$M[F(P_i(I_i)), F(P_j(I_j))] \quad (1)$$

where I_i and I_j are two face images, respectively; P stands for data processing to handle intra-personal variations, such as poses, illuminations, expressions and occlusions; F denotes feature extraction, which encodes the identity information; and M means a face matching algorithm used to compute similarity scores.

1) *Face Processing*: Although deep-learning-based approaches have been widely used due to their powerful representation, Ghazi et al. [52] proved that various conditions, such as poses, illuminations, expressions and occlusions, still affect the performance of deep FR and that face processing is beneficial, particularly for poses. Since pose variation is widely regarded as a major challenge in automatic FR applications, we mainly summarize the deep methods of face processing for poses in this paper. Other variations can be solved by similar methods.

The face processing methods are categorized as “one-to-many augmentation” and “many-to-one normalization”, as shown in Table I.

- “One-to-many augmentation”: generating many patches or images of the pose variability from a single image to enable deep networks to learn pose-invariant representations.
- “Many-to-one normalization”: recovering the canonical view of face images from one or many images of a

nonfrontal view; then, FR can be performed as if it were under controlled conditions.

2) *Deep Feature Extraction: Network Architecture*. The architectures can be categorized as backbone and multiple networks, as shown in Table II. Inspired by the extraordinary success on the ImageNet [138] challenge, the typical CNN architectures, such as AlexNet, VGGNet, GoogleNet, ResNet and SENet [94], [149], [158], [65], [75], are introduced and widely used as the baseline model in FR (directly or slightly modified). In addition to the mainstream, there are still some novel architectures designed for FR to improve efficiency. Moreover, when adopting backbone networks as basic blocks, FR methods often train multiple networks with multiple inputs or multiple tasks. One network is for one type of input or one type of task. Hu et al. [73] shows that it provides an increase in performance after accumulating the results of multiple networks.

Loss Function. The softmax loss is commonly used as the supervision signal in object recognition, and it encourages the separability of features. However, for FR, when intra-variations could be larger than inter-differences, the softmax loss is not sufficiently effective for FR. Many works focus on creating novel loss functions to make features not only more separable but also discriminative, as shown in Table III.

- Euclidean-distance-based loss: compressing intra-variance and enlarging inter-variance based on Euclidean distance.
- angular/cosine-margin-based loss: learning discriminative face features in terms of angular similarity, leading to potentially larger angular/cosine separability between learned features.
- softmax loss and its variations: directly using softmax loss or modifying it to improve performance, e.g., L2 normalization on features or weights as well as noise injection.

3) *Face Matching*: After the deep networks are trained with massive data and an appropriate loss function, each of the test images is passed through the networks to obtain a deep feature representation. Once the deep features are extracted, most methods directly calculate the similarity between two features using cosine distance or L2 distance; then, the nearest neighbor (NN) and threshold comparison are used for both identification and verification tasks. In addition to these, other methods are introduced to postprocess the deep features and perform the face matching efficiently and accurately, such as metric learning, sparse-representation-based classifier (SRC), and so forth.

To sum up, we present the various modules of FR and their commonly-used methods in Fig. 4 to help readers to get a view of the whole FR.

III. NETWORK ARCHITECTURE AND TRAINING LOSS

As there are billions of human faces in the earth, real-world FR can be regarded as an extremely fine-grained object classification task. For most applications, it is difficult to include the candidate faces during the training stage, which makes FR become a “zero-shot” learning task. Fortunately,

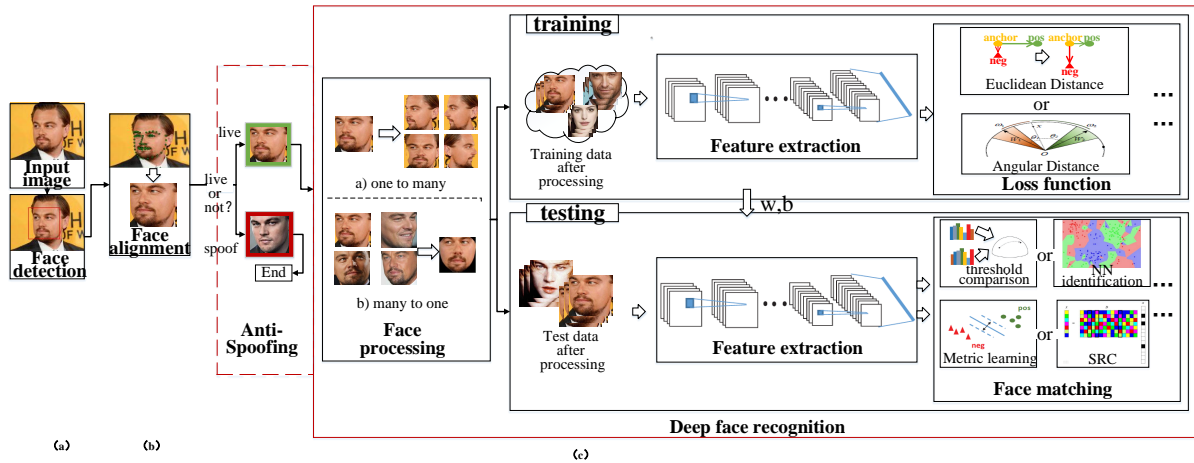


Fig. 3. Deep FR system with face detector and alignment. First, a face detector is used to localize faces. Second, the faces are aligned to normalized canonical coordinates. Third, the FR module is implemented. In FR module, face anti-spoofing recognizes whether the face is live or spoofed; face processing is used to handle recognition difficulty before training and testing; different architectures and loss functions are used to extract discriminative deep feature when training; face matching methods are used to do feature classification when the deep feature of testing data are extracted.

TABLE I
DIFFERENT DATA PREPROCESSING APPROACHES

Data processing	Brief Description	Subsettings
one to many	generating many patches or images of the pose variability from a single image	3D model [116], [114], [136], [137], [48] [57], [162], [161]
		2D deep model [242], [230], [148]
		data augmentation [105], [239], [46] [185], [152], [153], [157], [167]
many to one	recovering the canonical view of face images from one or many images of nonfrontal view	SAE [85], [227], [203]
		CNN [241], [243], [76], [35], [209]
		GAN [78], [163], [37], [212]

TABLE II
DIFFERENT NETWORK ARCHITECTURES OF FR

Network Architectures	Subsettings
backbone network	mainstream architectures: AlexNet [140], [139], [144], VGGNet [123], [116], [224], GoogleNet [204], [144], ResNet [106], [224], SENet [20]
	special architectures [187], [188], [157], [34], [194]
	joint alignment-representation architectures [64], [186], [237], [29]
multiple networks	multipose [87], [115], [211], [175], multipatch [105], [239], [46], [155], [156], [152] [185], multitask [131]

TABLE III
DIFFERENT LOSS FUNCTIONS FOR FR

Loss Functions	Brief Description
Euclidean-distance-based loss	compressing intra-variance and enlarging inter-variance based on Euclidean distance. [152], [185], [153], [181], [191], [224], [144], [123], [140], [139], [105], [28]
angular/cosine-margin-based loss	making learned features potentially separable with larger angular/cosine distance. [107], [106], [170], [38], [172], [108]
softmax loss and its variations	modifying the softmax loss to improve performance. [129], [171], [61], [111] [128], [23], [62]

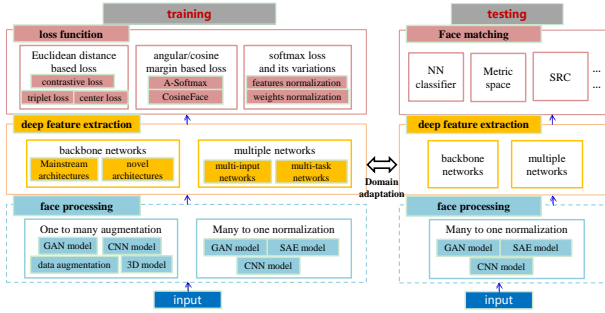


Fig. 4. The different components of FR. Some important methods of data processing, architecture, loss function and face matching are listed

since all human faces share a similar shape and texture, the representation learned from a small proportion of faces can generalize well to the rest. A straightforward way is to include as many IDs as possible in the training set. For example, Internet giants such as Facebook and Google have reported their deep FR system trained by $10^6 - 10^7$ IDs [144], [160]. Unfortunately, these personal datasets, as well as prerequisite GPU clusters for distributed model training, are not accessible for academic community. Currently, public available training databases for academic research consist of only $10^3 - 10^5$ IDs.

Instead, academic community make effort to design effective loss functions and adopt deeper architectures to make deep features more discriminative using the relatively small training data sets. For instance, the accuracy of most popular LFW benchmark has been boosted from 97% to above 99.8% in the pasting four years, as enumerated in Table IV. In this section, we survey the research efforts on different loss functions and network architecture that have significantly improved deep FR methods.

A. Evolution of Discriminative Loss Functions

Inheriting from the object classification network such as AlexNet, the initial Deepface [160] and DeepID [156] adopted cross-entropy based softmax loss for feature learning. After that, people realized that the softmax loss is not sufficient by itself to learn feature with large margin, and more researchers began to explore discriminative loss functions for enhanced generalization ability. This become the hottest research topic for deep FR research, as illustrated in Fig. 5. Before 2017, Euclidean-distance-based loss played an important role; In 2017, angular/cosine-margin-based loss as well as feature and weight normalization became popular. It should be noted that, although some loss functions share similar basic idea, the new one is usually designed to facilitate the training procedure by easier parameter or sample selection.

1) *Euclidean-distance-based Loss* : Euclidean-distance-based loss is a metric learning method[193], [179] that embeds images into Euclidean space and compresses intra-variance and enlarges inter-variance. The contrastive loss and the triplet loss are the commonly used loss functions. The contrastive loss [185], [152], [153], [157], [206] requires face image pairs and

then pulls together positive pairs and pushes apart negative pairs.

$$\mathcal{L} = y_{ij} \max(0, \|f(x_i) - f(x_j)\|_2 - \epsilon^+) + (1 - y_{ij}) \max(0, \epsilon^- - \|f(x_i) - f(x_j)\|_2) \quad (2)$$

where $y_{ij} = 1$ means x_i and x_j are matching samples and $y_{ij} = -1$ means non-matching samples. $f(\cdot)$ is the feature embedding, ϵ^+ and ϵ^- control the margins of the matching and non-matching pairs respectively. DeepID2 [185] combined the face identification (softmax) and verification (contrastive loss) supervisory signals to learn a discriminative representation, and joint Bayesian (JB) was applied to obtain a robust embedding space. Extending from DeepID2 [185], DeepID2+ [152] increased the dimension of hidden representations and added supervision to early convolutional layers, while DeepID3 [153] further introduced VGGNet and GoogleNet to their work. However, the main problem with the contrastive loss is that the margin parameters are often difficult to choose.

Contrary to contrastive loss that considers the absolute distances of the matching pairs and non-matching pairs, triplet loss considers the relative difference of the distances between them. Along with FaceNet [144] proposing by Google, Triplet loss [144], [123], [139], [140], [105], [46] was introduced into FR. It requires the face triplets, and then it minimizes the distance between an anchor and a positive sample of the same identity and maximizes the distance between the anchor and a negative sample of a different identity. FaceNet made $\|f(x_i^a) - f(x_i^p)\|_2^2 + \alpha < -\|f(x_i^a) - f(x_i^n)\|_2^2$ using hard triplet face samples, where x_i^a , x_i^p and x_i^n are the anchor, positive and negative samples, respectively; α is a margin; and $f(\cdot)$ represents a nonlinear transformation embedding an image into a feature space. Inspired by FaceNet [144], TPE [139] and TSE [140] learned a linear projection W to construct triplet loss, where the former satisfied Eq. 3 and the latter followed Eq. 4. Other methods combine triplet loss with softmax loss [239], [105], [46], [36]. They first train networks with the softmax and then fine-tune them with triplet loss.

$$(x_i^a)^T W^T W x_i^p + \alpha < (x_i^a)^T W^T W x_i^n \quad (3)$$

$$(x_i^a - x_i^p)^T W^T W (x_i^a - x_i^p) + \alpha < (x_i^a - x_i^n)^T W^T W (x_i^a - x_i^n) \quad (4)$$

However, the contrastive loss and triplet loss occasionally encounter training instability due to the selection of effective training samples, some paper begun to explore simple alternatives. Center loss [181] and its variant [224], [39], [191] is a good choice to compresses intra-variance. In [181], the center loss learned a center for each class and penalized the distances between the deep features and their corresponding class centers. This loss can be defined as follows:

$$\mathcal{L}_C = \frac{1}{2} \sum_{i=1}^m \|x_i - c_{y_i}\|_2^2 \quad (5)$$

where x_i denotes the i th deep feature belonging to the y_i th class and c_{y_i} denotes the y_i th class center of deep features. To handle the long-tailed data, A range loss [224] is used to minimize k greatest range's harmonic mean values in one class and maximize the shortest inter-class distance within one

TABLE IV
THE ACCURACY OF DIFFERENT VERIFICATION METHODS ON THE LFW DATASET.

Method	Public. Time	Loss	Architecture	Number of Networks	Training Set	Accuracy±Std(%)
DeepFace [160]	2014	softmax	Alexnet	3	Facebook (4.4M,4K)	97.35±0.25
DeepID2 [152]	2014	contrastive loss	Alexnet	25	CelebFaces+ (0.2M,10K)	99.15±0.13
DeepID3 [153]	2015	contrastive loss	VGGNet-10	50	CelebFaces+ (0.2M,10K)	99.53±0.10
FaceNet [144]	2015	triplet loss	GoogleNet-24	1	Google (500M,10M)	99.63±0.09
Baidu [105]	2015	triplet loss	CNN-9	10	Baidu (1.2M,18K)	99.77
VGGface [123]	2015	triplet loss	VGGNet-16	1	VGGface (2.6M,2.6K)	98.95
light-CNN [188]	2015	softmax	light CNN	1	MS-Celeb-1M (8.4M,100K)	98.8
Center Loss [181]	2016	center loss	Lenet+-7	1	CASIA-WebFace, CACD2000, Celebrity+ (0.7M,17K)	99.28
L-softmax [107]	2016	L-softmax	VGGNet-18	1	CASIA-WebFace (0.49M,10K)	98.71
Range Loss [224]	2016	range loss	VGGNet-16	1	MS-Celeb-1M, CASIA-WebFace (5M,100K)	99.52
L2-softmax [129]	2017	L2-softmax	ResNet-101	1	MS-Celeb-1M (3.7M,58K)	99.78
Normface [171]	2017	contrastive loss	ResNet-28	1	CASIA-WebFace (0.49M,10K)	99.19
CoCo loss [111]	2017	CoCo loss	-	1	MS-Celeb-1M (3M,80K)	99.86
vMF loss [62]	2017	vMF loss	ResNet-27	1	MS-Celeb-1M (4.6M,60K)	99.58
Marginal Loss [39]	2017	marginal loss	ResNet-27	1	MS-Celeb-1M (4M,80K)	99.48
SphereFace [106]	2017	A-softmax	ResNet-64	1	CASIA-WebFace (0.49M,10K)	99.42
CCL [128]	2018	center invariant loss	ResNet-27	1	CASIA-WebFace (0.49M,10K)	99.12
AMS loss [170]	2018	AMS loss	ResNet-20	1	CASIA-WebFace (0.49M,10K)	99.12
Cosface [172]	2018	cosface	ResNet-64	1	CASIA-WebFace (0.49M,10K)	99.33
Arcface [38]	2018	arcface	ResNet-100	1	MS-Celeb-1M (3.8M,85K)	99.83
Ring loss [235]	2018	Ring loss	ResNet-64	1	MS-Celeb-1M (3.5M,31K)	99.50

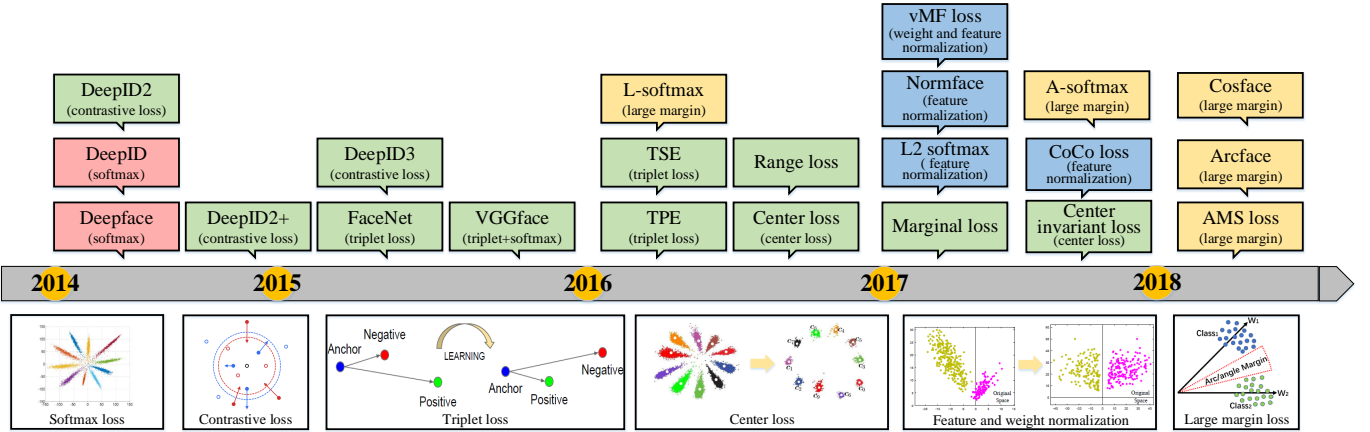


Fig. 5. The development of loss functions. It marks the beginning of deep FR that Deepface [160] and DeepID [156] were introduced in 2014. After that, Euclidean-distance-based loss always played the important role in loss function, such as contrastive loss, triplet loss and center loss. In 2016 and 2017, L-softmax [107] and A-softmax [106] further promoted the development of the large-margin feature learning. In 2017, feature and weight normalization also began to show excellent performance, which leads to the study on variations of softmax. Red, green, blue and yellow rectangles represent deep methods with softmax, Euclidean-distance-based loss, angular/cosine-margin-based loss and variations of softmax, respectively.

batch, while Wu et al. [191] proposed a center-invariant loss that penalizes the difference between each center of classes. Deng et al. [39] selected the farthest intra-class samples and the nearest inter-class samples to compute a margin loss. However, the center loss and its variant suffer from massive GPU memory consumption on the classification layer, and prefer balanced and sufficient training data for each identity.

2) *Angular/cosine-margin-based Loss* : In 2017, people had a deeper understanding of loss function in deep FR and thought that samples should be separated more strictly to avoid misclassifying the difficult samples. Angular/cosine-margin-based loss [107], [106], [170], [38], [108] is proposed to make learned features potentially separable with a larger angular/cosine distance. Liu et al. [107] reformulated the original softmax loss into a large-margin softmax (L-Softmax) loss,

which requires $\|W_1\| \|x\| \cos(m\theta_1) > \|W_2\| \|x\| \cos(\theta_2)$, where m is a positive integer introducing an angular margin, W is the weight of the last fully connected layer, x denotes the deep feature and θ is the angle between them. Due to the non-monotonicity of the cosine function, a piece-wise function is applied in L-softmax to guarantee the monotonicity. The loss function is defined as follows:

$$\mathcal{L}_i = -\log \left(\frac{e^{\|W_{y_i}\| \|x_i\| \varphi(\theta_{y_i})}}{e^{\|W_{y_i}\| \|x_i\| \varphi(\theta_{y_i})} + \sum_{j \neq y_i} e^{\|W_{y_i}\| \|x_i\| \cos(\theta_j)}} \right) \quad (6)$$

where

$$\varphi(\theta) = (-1)^k \cos(m\theta) - 2k, \theta \in \left[\frac{k\pi}{m}, \frac{(k+1)\pi}{m} \right] \quad (7)$$

Due to L-Softmax has difficulty converging, softmax loss is always combined to facilitate and ensure the convergence, and the weight is controlled by a dynamic hyper-parameter λ . With the additional softmax loss, the loss function is changed into: $f_{y_i} = \frac{\lambda \|W_{y_i}\| \|x_i\| \cos(\theta_{y_i}) + \|W_{y_i}\| \|x_i\| \varphi(\theta_{y_i})}{1 + \lambda}$. Based on L-Softmax, A-Softmax loss [106] further normalized the weight W by its L2 norm ($\|W\| = 1$) such that the normalized vector will lie on a hypersphere, and then the discriminative face features can be learned on a hypersphere manifold with an angular margin (Fig. 6). Liu et al. [108] introduced a deep hyperspherical convolution network (SphereNet) that adopts hyperspherical convolution as its basic convolution operator and is supervised by angular-margin-based loss. To overcome the optimization difficulty of L-Softmax and A-Softmax, which incorporate the angular margin in a multiplicative manner, ArcFace [38] and CosineFace [170], AMS loss [172] respectively introduced an additive angular/cosine margin $\cos(\theta + m)$ and $\cos\theta - m$. They are extremely easy to implement without tricky hyper-parameters λ , and are more clear and able to converge without the softmax supervision. The decision boundaries under the binary classification case are given in Table VII. Compared to Euclidean-distance-based loss, angular/cosine-margin-based loss explicitly adds discriminative constraints on a hypersphere manifold, which intrinsically matches the prior that human face lies on a manifold; but Wang et al. [169] showed that angular/cosine-margin-based loss, which used to achieve a better result on a clean dataset, is vulnerable to noise and becomes worse than Center loss and Softmax in the high-noise region. (Fig. 7)

TABLE V
DECISION BOUNDARIES FOR CLASS 1 UNDER BINARY CLASSIFICATION CASE, WHERE \hat{x} IS THE NORMALIZED FEATURE. [38]

Loss Functions	Decision Boundaries
Softmax	$(W_1 - W_2)x + b_1 - b_2 = 0$
L-Softmax [107]	$\ x\ (\ W_1\ \cos(m\theta_1) - \ W_2\ \cos(\theta_2)) > 0$
A-Softmax [106]	$\ x\ (\cos m\theta_1 - \cos\theta_2) = 0$
CosineFace [170]	$\hat{x} (\cos\theta_1 - m - \cos\theta_2) = 0$
ArcFace [38]	$\hat{x} (\cos(\theta_1 + m) - \cos\theta_2) = 0$

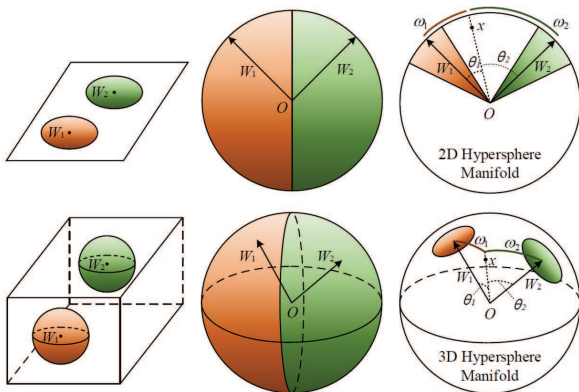


Fig. 6. Geometry interpretation of A-Softmax loss. [106]

3) *Softmax Loss and its Variations* : In 2017, In addition to reformulating softmax loss into an angular/cosine-margin-based loss as mentioned above, there are also many works

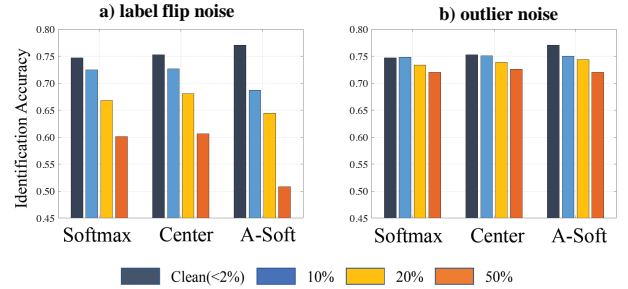


Fig. 7. 1:1M rank-1 identification results on MegaFace benchmark: (a) introducing label flips to training data, (b) introducing outliers to training data. [169]

focusing on modifying it in detail. Normalization of feature or weight in softmax loss is one of the strategies, which can be written as follows:

$$\hat{W} = \frac{W}{\|W\|}, \hat{x} = \alpha \frac{x}{\|x\|} \quad (8)$$

where α is a scaling parameter. Scaling x to a fixed radius α is important, as [171] proved that normalizing the features and weights to 1 will make the softmax loss become trapped at a very high value on the training set. Feature and weight normalization are just effective tricks and should be implemented with other loss functions.

In [106], [170], [38], [108], the loss functions normalized the weights only and trained with angular/cosine margin to make the learned features be discriminative. In contrast, some works, such as [129], [61], adopted feature normalization only to overcome the bias to the sample distribution of the softmax. Based on the observation of [122] that the L2-norm of features learned using the softmax loss is informative of the quality of the face, L2-softmax [129] enforced all the features to have the same L2-norm by feature normalization such that similar attention is given to good quality frontal faces and blurry faces with extreme pose. Rather than scaling parameter α , Hasnat et al. [61] normalized features with $\hat{x} = \frac{x - \mu}{\sqrt{\sigma^2}}$, where μ and σ^2 are the mean and variance. Ring loss [235] encouraged norm of samples being value R (a learned parameter) rather than explicit enforcing through a hard normalization operation. Moreover, normalizing both features and weights [171], [111], [62] has become a common strategy in softmax. In [171], Wang et al. explained the necessity of this normalization operation from both analytic and geometric perspectives. After normalizing features and weights, CoCo loss [111] optimized the cosine distance among data features, and [62] used the von Mises-Fisher (vMF) mixture model as the theoretical basis to develop a novel vMF mixture loss and its corresponding vMF deep features.

In addition to normalization, there are also other strategies to modify softmax; for example, Chen et al. [23] proposed a noisy softmax to mitigate early saturation by injecting annealed noise in softmax.

B. Evolution of Network Architecture

1) *Backbone Network* : **Mainstream architectures.** The commonly used network architectures of deep FR have always

followed those of deep object classification and evolved from AlexNet to SENet rapidly. We present the most influential architectures that have shaped the current state-of-the-art of deep object classification and deep FR in chronological order¹ in Fig. 8.

In 2012, AlexNet [94] was reported to achieve state-of-the-art recognition accuracy in the ImageNet large-scale visual recognition competition (ILSVRC) 2012, exceeding the previous best results by a large margin. AlexNet consists of five convolutional layers and three fully connected layers, and it also integrates various techniques, such as rectified linear unit (ReLU), dropout, data augmentation, and so forth. ReLU was widely regarded as the most essential component for making deep learning possible. Then, in 2014, VGGNet [149] proposed a standard network architecture that used very small 3×3 convolutional filters throughout and doubled the number of feature maps after the 2×2 pooling. It increased the depth of the network to 16-19 weight layers, which further enhanced the flexibility to learn progressive nonlinear mappings by deep architectures. In 2015, the 22-layer GoogleNet [158] introduced an “inception module” with the concatenation of hybrid feature maps, as well as two additional intermediate softmax supervised signals. It performs several convolutions with different receptive fields (1×1 , 3×3 and 5×5) in parallel, and it concatenates all feature maps to merge the multi-resolution information. In 2016, ResNet [65] proposed making layers learn a residual mapping with reference to the layer inputs $\mathcal{F}(x) := \mathcal{H}(x) - x$ rather than directly learning a desired underlying mapping $\mathcal{H}(x)$ to ease the training of very deep networks (up to 152 layers). The original mapping is recast into $\mathcal{F}(x) + x$ and can be realized by “shortcut connections”. As the champion of ILSVRC 2017, SENet [75] introduced a “squeeze-and-excitation” (SE) block, that adaptively recalibrates channel-wise feature responses by explicitly modelling interdependencies between channels. These blocks can be integrated with modern architectures, such as ResNet, and improves their representational power. With the evolved architectures and advanced training techniques, such as batch normalization (BN), the network becomes deeper and the training becomes more controllable, and the performance of object classification is continually improving. We present these mainstream architectures in Fig. 9.

Motivated the substantial progress in object classification, the deep FR community follows these mainstream architectures step by step. In 2014, DeepFace [160] was the first to use a nine-layer CNN with several locally connected layers. With 3D alignment for data processing, it reaches an accuracy of 97.35% on LFW. In 2015, FaceNet [144] used a large private dataset to train a GoogleNet. It adopted a triplet loss function based on triplets of roughly aligned matching/nonmatching face patches generated by a novel online triplet mining method and achieved good performance (99.63%). In the same year, VGGface [123] designed a procedure to collect a large-scale dataset from the Internet. It trained the VGGNet on this dataset and then fine-tuned the networks via a triplet loss function similar to FaceNet. VGGface obtains an accuracy of 98.95%.

In 2017, SphereFace [106] used a 64-layer ResNet architecture and proposed the angular softmax (A-Softmax) loss to learn discriminative face features with angular margin (99.42%). In the end of 2017, a new large-scale face dataset, namely VGGFace2 [20], was introduced, which consists of large variations in pose, age, illumination, ethnicity and profession. Cao et al. first trained a SENet with MS-celeb-1M dataset[59] and then fine-tuned the model with VGGface2, and achieved state-of-the-art performance on the IJB-A [93] and IJB-B [182].

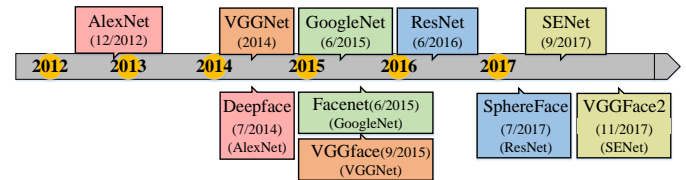


Fig. 8. The top row presents the typical network architectures in object classification, and the bottom row describes the well-known algorithms of deep FR that use the typical architectures and achieve good performance. The same color rectangles mean the same architecture. It is easy to find that the architectures of deep FR have always followed those of deep object classification and evolved from AlexNet to SENet rapidly.

Special architectures. In addition, there are some special architectures in FR. Light CNN [188], [187] proposed a max-feature-map (MFM) activation function that introduces the concept of maxout in the fully connected layer to CNN. The MFM obtains a compact representation and reduces the computational cost. Inspired by [103], Chowdhury et al. [34] applied the bilinear CNN (B-CNN) in FR. The outputs at each location of two CNNs are combined (using outer product) and are then average pooled to obtain the bilinear feature representation. Han et.al [60] proposed a novel contrastive convolution, consists of a trunk CNN and a kernel generator, which is beneficial owing to its dynamistic generation of contrastive kernels and distinct characteristics based on the pair of faces being compared. Kang et. al [88] proposed a pairwise relational network (PRN) to capture unique relations within same identity and discriminative relations among different identities from a pair of local appearance patches using relation feature obtained by multi-layer perceptron (MLP) and a face identity state feature. Sun et al. [157] proposed sparsifying deep networks iteratively from the previously learned denser models based on a weight selection criterion. Conditional convolutional neural network (c-CNN) [194] dynamically activated sets of kernels according to modalities of samples. Although the light-weight CNNs for mobile devices, such as SqueezeNet, MobileNet, ShuffleNet and Xception [79], [72], [33], [226], are still not widely used in FR, they have potential and deserve more attention.

Joint alignment-representation networks Recently, an end-to-end system [64], [186], [237], [29] was proposed to jointly train FR with several modules (face detection, alignment, and so forth) together. Compared to the existing methods in which each module is generally optimized separately according to different objectives, this end-to-end system optimizes each module according to the recognition objective, leading to more adequate and robust inputs for the recognition model. For example, inspired by spatial transformer [80],

¹The time we present is when the paper was published.

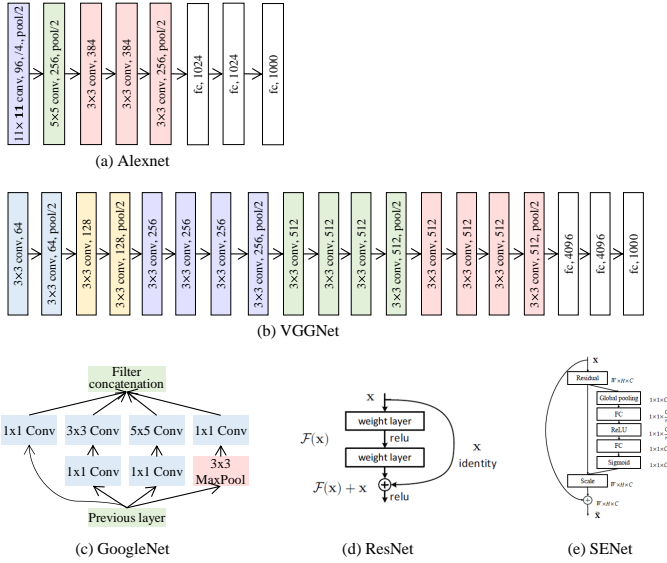


Fig. 9. The architecture of Alexnet, VGGNet, GoogleNet, ResNet, SENet.

Hayat et al. [64] proposed a CNN-based data-driven approach that learns to simultaneously register and represent faces (Fig. 19), while Wu et al. [186] designed a novel recursive spatial transformer (ReST) module for CNN allowing face alignment and recognition to be jointly optimized.

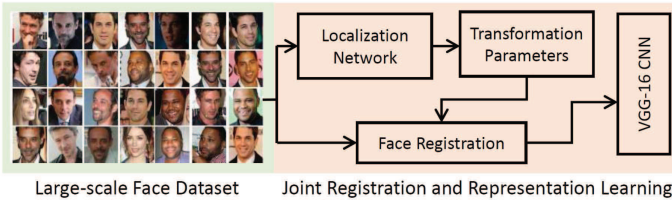


Fig. 10. Joint face registration and representation. [64]

2) **Multiple Networks : Multi-input networks.** Corresponding to “one-to-many augmentation”, which generate multiple images of different patches or poses, the architectures also change into multiple networks for different image inputs. In [105], [239], [46], [155], [156], [152], [185], multiple networks are built after different numbers of face patches are cropped, and then one network handles one type of patch for representation extraction. Other papers [115], [87], [175] used multiple networks to handle images of different poses. For example, Masi et al. [115] adjusted the pose to frontal (0°), half-profile (40°) and full-profile views (75°) and then addressed pose variation by multiple pose networks. A multi-view deep network (MvDN) [87] consists of view-specific subnetworks and common subnetworks; the former removes view-specific variations, and the latter obtains common representations. Wang et al. [175] used coupled SAE for cross-view FR.

Multi-task learning networks. The other form of multiple networks is for multi-task learning, where identity classification is the main task, and the side tasks are pose, illumination, and expression estimations, among others. In these networks, the lower layers are shared among all the tasks, and the higher

layers are disentangled into multiple networks to generate the task-specific outputs. In [131], the task-specific subnetworks are branched out to learn face detection, face alignment, pose estimation, gender recognition, smile detection, age estimation and FR. Yin et al. [211] proposed automatically assigning the dynamic loss weights for each side task. Peng et al. [125] used a feature reconstruction metric learning to disentangle a CNN into subnetworks for identity and pose (Fig. 11).

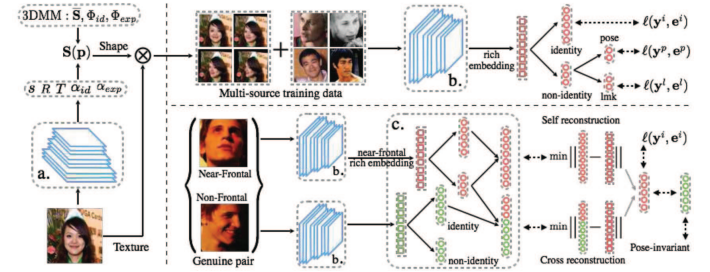


Fig. 11. Reconstruction-based disentanglement for pose-invariant FR. [125]

C. Face Matching by deep features

During testing, the cosine distance and L2 distance are generally employed to measure the similarity between the deep features x_1 and x_2 ; then, threshold comparison and the nearest neighbor (NN) classifier are used to make decision for verification and identification. In addition to these common methods, there are some other explorations.

1) **Face verification:** Metric learning, which aims to find a new metric to make two classes more separable, can also be used for face matching based on extracted deep features. The JB [25] model is a well-known metric learning method [185], [152], [153], [156], [206], and Hu et al. [73] proved that it can improve the performance greatly. In the JB model, a face feature x is modeled as $x = \mu + \varepsilon$, where μ and ε are identity and intra-personal variations, respectively. The similarity score $r(x_1, x_2)$ can be represented as follows:

$$r(x_1, x_2) = \log \frac{P(x_1, x_2 | H_I)}{P(x_1, x_2 | H_E)} \quad (9)$$

where $P(x_1, x_2 | H_I)$ is the probability that two faces belong to the same identity and $P(x_1, x_2 | H_E)$ is the probability that two faces belong to different identities.

2) **Face Identification:** After cosine distance was computed, Cheng et al. [30] proposed a heuristic voting strategy at the similarity score level for robust multi-view combination of multiple CNN models and won first place in challenge2 of MS-celeb-1M 2017. In [205], Yang et al. extracted the local adaptive convolution features from the local regions of the face image and used the extended SRC for FR with a single sample per person. Guo et al. [56] combined deep features and the SVM classifier to recognize all the classes. Based on deep features, Wang et al. [167] first used product quantization (PQ) [82] to directly retrieve the top-k most similar faces and re-ranked these faces by combining similarities from deep features and the COTS matcher [54]. In addition, Softmax can be also used in face matching when the identities of training

set and test set overlap. For example, in challenge2 of MS-celeb-1M, Ding et al. [236] trained a 21,000-class softmax classifier to directly recognize faces of one-shot classes and normal classes after augmenting feature by a conditional GAN; Guo et al. [58] trained the softmax classifier combined with underrepresented-classes promotion (UP) loss term to enhance the performance.

When the distribution of training data and testing data are the same, the face matching methods mentioned above are effective. However, there is always a distribution change or domain shift between two domains that can degrade the performance. Transfer learning [120], [174] has recently been introduced for deep FR, which utilizes data in relevant source domains (training data) to execute FR in a target domain (testing data). Sometimes, it will be used to help face matching, for example [36], [195] adopted template adaptation, which is a form of transfer learning to the set of media in a template, by combining CNN features with template-specific linear SVMs. But most of the time, it is not enough to do transfer learning only at face matching. Transfer learning should be embedded in deep models to learn more transferable representations. Kan et al. [86] proposed a bi-shifting autoencoder network (BAE) for domain adaptation across view angle, ethnicity, and imaging sensor; while Luo et al. [244] utilized the multi-kernels maximum mean discrepancy (MMD) for the same purpose. Sohn et al. [150] used adversarial learning [165] to transfer knowledge of still image FR to video FR. Fine-tuning the CNN parameters from a prelearned model using a target training dataset is a particular form of transfer learning. It is commonly employed by numerous methods [4], [168], [28].

IV. FACE PROCESSING FOR TRAINING AND RECOGNITION

When we look into the development of methods of face processing in chronological order as shown in Fig. 12, there are different mainstreams every year. In 2014 and 2015, most papers attempted to perform face processing by SAE model and CNN model; while 3D model played an important role in 2016. GAN [53] has drawn substantial attention from the deep learning and computer vision community since it was first introduced by Goodfellow et al. It can be used in different fields and was also introduced into face processing. GANs showed extraordinary talents in 2017, it can perform not only “one-to-many augmentation” but also “many-to-one normalization”, and it broke the limit that face synthesis should be done under supervised way. Although GAN has not been widely used in face processing for training and recognition, it has great potential, for example, Dual-Agent GANs (DA-GAN) [230] won the 1st places on verification and identification tracks in the NIST IJB-A 2017 FR competitions.

A. One-to-Many Augmentation

Collecting a large database is extremely expensive and time consuming. The methods of “one-to-many augmentation” can mitigate the challenges of data collection, and they can be used to augment not only training data but also the gallery of test data. we categorized them into four classes: data augmentation, 3D model, CNN model and GAN model.

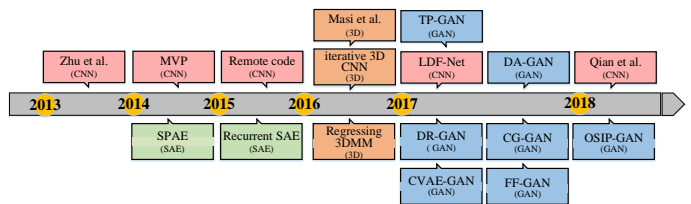


Fig. 12. The development of different methods of face processing. Red, green, orange and blue rectangles represent CNN model, SAE model, 3D model and GAN model, respectively.

Data augmentation. Common data augmentation methods consist of photometric transformations [149], [94] and geometric transformations, such as oversampling (multiple patches obtained by cropping at different scales) [94], mirroring [201], and rotating [192] the images. Recently, data augmentation has been widely used in deep FR algorithms [105], [239], [46], [185], [152], [153], [157], [167]. for example, Sun et al. [152] cropped 400 face patches varying in positions, scales, and color channels and mirrored the images. In [105], seven CNNs with the same structure were used on seven overlapped image patches centered at different landmarks on the face region.

3D model. 3D face reconstruction is also a way to enrich the diversity of training data. There is a large number of papers about this domain, but we only focus on the 3D face reconstruction using deep methods or used for deep FR. In [116], Masi et al. generated face images with new intra-class facial appearance variations, including pose, shape and expression, and then trained a 19-layer VGGNet with both real and augmented data. [114] used generic 3D faces and rendered fixed views to reduce much of the computational effort. Richardson et al. [136] employed an iterative CNN by using a secondary input channel to represent the previous network’s output as an image for reconstructing a 3D face (Fig. 13). Dou et al. [48] used a multi-task CNN to divide 3D face reconstruction into neutral 3D reconstruction and expressive 3D reconstruction. Tran et al. [162] directly regressed 3D morphable face model (3DMM) [16] parameters from an input photo by a very deep CNN architecture. An et al. [217] synthesized face images with various poses and expressions using the 3DMM method, then reduced the gap between synthesized data and real data with the help of MMD.

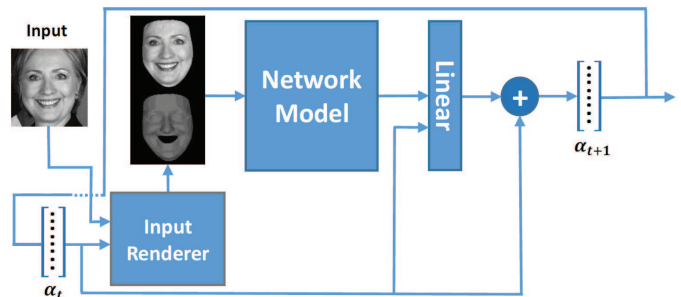


Fig. 13. Iterative CNN network for reconstructing a 3D face. [136]

CNN model. Rather than reconstructing 3D models from a 2D image and projecting it back into 2D images of different poses, CNN models can generate 2D images directly. In the

multi-view perceptron (MVP) [242], the deterministic hidden neurons learn the identity features, while the random hidden neurons capture the view features. By sampling different random neurons, the face images of different poses are synthesized. Similar to [209], Qian et al. [208] used 7 Recon codes to rotate faces into 7 different poses, and proposed a novel type of unpair-supervised way to learn the face variation representation instead of supervising by Recon codes.

GAN model. After using a 3D model to generate profile face images, DA-GAN [230] refined the images by a GAN, which combines prior knowledge of the data distribution and knowledge of faces (pose and identity perception loss). CVAE-GAN [11] combined a variational auto-encoder with a GAN for augmenting data, and took advantages of both statistic and pairwise feature matching to make the training process converge faster and more stably. In addition to synthesizing diverse faces from noise, some papers also explore to disentangle the identity and variation, and synthesize new faces by exchanging them between different people. In CG-GAN [178], a generator directly resolves each representation of input image into a variation code and a identity code and regroups these codes for cross-generating, while a discriminator ensures the reality of generated images. Bao et al. [12] extracted identity representation of one input image and attribute representation of any other input face image, then synthesized new faces from recombining these representations. This work shows superior performance in generating realistic and identity preserving face images, even for identities outside the training dataset. Unlike previous methods that treat classifier as a spectator, FaceID-GAN [214] proposed a three-player GAN where the classifier cooperates together with the discriminator to compete with the generator from two different aspects, facial identity and image quality respectively.

B. Many-to-One Normalization

In contrast to “one-to-many augmentation”, the methods of “many-to-one normalization” produce frontal faces and reduce appearance variability of test data to make faces align and compare easily. It can be categorized as SAE, CNN and GAN models.

SAE. The proposed stacked progressive autoencoders (SPAЕ) [85] progressively map the nonfrontal face to the frontal face through a stack of several autoencoders. In [203], a novel recurrent convolutional encoder-decoder network combined with shared identity units and recurrent pose units can render rotated objects instructed by control signals at each time step. Zhang et al. [227] built a sparse many-to-one encoder by setting frontal face and multiple random faces as the target values.

CNN. Zhu et al. [241] extracted face identity-preserving features to reconstruct face images in the canonical view using a CNN that consists of a feature extraction module and a frontal face reconstruction module. Zhu et al. [243] selected canonical-view images according to the face images’ symmetry and sharpness and then adopted a CNN to recover the frontal view images by minimizing the reconstruction loss error. Yim et al. [209] proposed a multi-task network that

can rotate an arbitrary pose and illumination image to the target-pose face image by utilizing the user’s remote code. [76] transformed nonfrontal face images to frontal images according to the displacement field of the pixels between them. [238] proposed a novel non-rigid face rectification method by local homography transformations, and regularized it by imposing natural frontal face distribution with a denoising autoencoder.

GAN. [78] proposed a two-pathway generative adversarial network (TP-GAN) that contains four landmark-located patch networks and a global encoder-decoder network. Through combining adversarial loss, symmetry loss and identity-preserving loss, TP-GAN generates a frontal view and simultaneously preserves global structures and local details (Fig. 14). In a disentangled representation learning generative adversarial network (DR-GAN) [163], an encoder produces an identity representation, and a decoder synthesizes a face at the specified pose using this representation and a pose code. Yin et al. [212] incorporated 3DMM into the GAN structure to provide shape and appearance priors to guide the generator to frontalization.

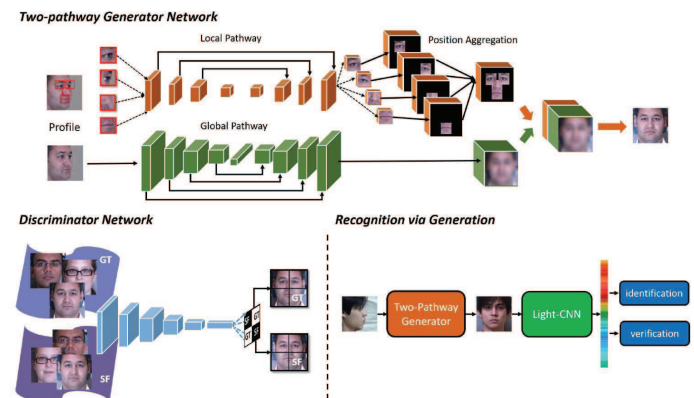


Fig. 14. General framework of TP-GAN. [78]

V. FACE DATABASES AND EVALUATION PROTOCOLS

In the past three decades, many face databases have been constructed with a clear tendency from small-scale to large-scale, from single-source to diverse-sources, and from lab-controlled to real-world unconstrained condition, as shown in Fig. 15. As the performance of some simple databases become saturated, e.g. LFW, more and more complex databases were continually developed to facilitate the FR research. It can be said without exaggeration that the development process of the face databases largely leads the direction of FR research. In this section, we review the development of major training and testing academic databases for the deep FR.

A. Large-scale training data sets and their label noise

The prerequisite of effective deep FR is a sufficiently large training dataset. Zhou et al. [239] suggested that large amounts of data with deep learning improve the performance of FR. The results of Megaface Challenge also revealed that premier deep FR methods were typically trained on data larger than 0.5M images and 20K people. The early works of deep FR were

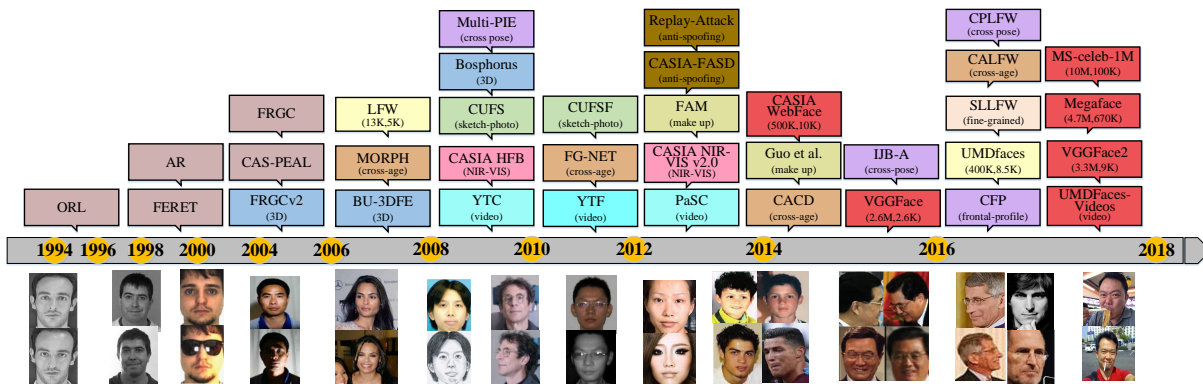


Fig. 15. The evolution of FR datasets. Before 2007, early work in FR focused on controlled and small-scale datasets. In 2007, LFW [77] dataset was introduced which marks the beginning of FR under unconstrained conditions. Since then, more testing databases with different tasks and scenes are designed. And in 2014, CASIA-Webface [206] provided the first widely-used public training dataset, large-scale training datasets begun to be hot topic. Red rectangles represent training datasets, and other color rectangles represent testing datasets with different task and scenes.

usually trained on private training datasets. Facebook’s Deepface [160] model was trained on 4M images of 4K people; Google’s FaceNet [144] was trained on 200M images of 3M people; DeepID serial models [156], [185], [152], [153] were trained on 0.2M images of 10K people. Although they reported ground-breaking performance at this stage, researchers cannot accurately reproduce or compare their models without public training datasets.

To address this issue, CASIA-Webface [206] provided the first widely-used public training dataset for the deep model training purpose, which consists of 0.5M images of 10K celebrities, collected from the web. Given its moderate size and easy usage, it has become a great resource for fair comparisons for academic deep models. However, its relatively small data and ID size may not be sufficient to reflect the power of many advanced deep learning methods. Currently, there have been more databases providing public available large-scale training dataset (Table VI), especially three databases with over 1M images, namely MS-Celeb-1M [59], VGGface2 [20], and Megaface [89], [119], and we summary some interesting findings about these training sets, as shown in Fig. 16.

These large training sets are expanded from depth or breadth. VGGface2 provides a large-scale training dataset of depth, which has limited number of subjects but many images for each subjects. The depth of dataset enforces the trained model to address a wide range intra-class variations, such as lighting, age, and pose; In contrast, MS-Celeb-1M and Mageface (Challenge 2) offers large-scale training datasets of breadth, which contains many subject but limited images for each subjects. The breadth of dataset ensures the trained model to cover the sufficiently variable appearance of various people. Cao et al. [20] conducted a systematic studies on model training using VGGface2 and MS-Celeb-1M, and found an optimal model by first training on MS-Celeb-1M (breadth) and then fine-tuning on VGGface2 (depth).

The utilization of long tail distribution is different among datasets. For example, in challenge 2 of MS-Celeb-1M, the novel set specially uses the tailed data to study low-shot learning; central part of the distribution is used by the challenge 1 of MS-Celeb-1M and images’ number is approximately limited to

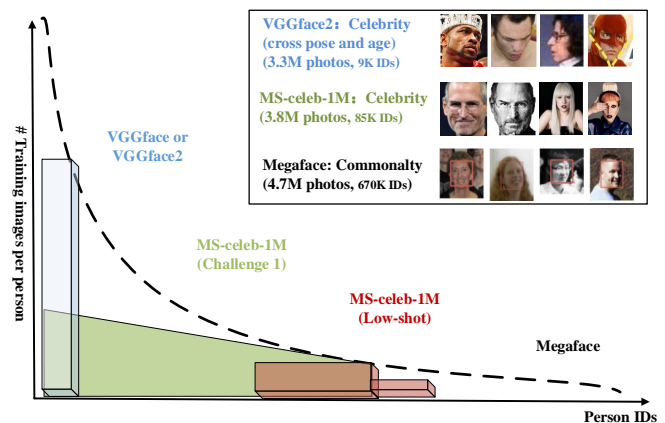


Fig. 16. The distribution of different large databases. The vertical axis displays number of images per person, and the horizontal axis shows person IDs.

100 for each celebrity; VGGface and VGGface2 only use the head part to construct deep databases; Megaface utilizes the whole distribution to contain as many images as possible, the minimal number of images is 3 per person and the maximum is 2469.

Data bias usually exists in most databases. One reason is that only partial distribution of face data is covered by each database. The other is that most datasets (VGGface2 and MS-celeb-1M) consist of celebrities on formal occasions: smiling, make-up, young, and beautiful. It is largely different from databases captured in the daily life (Megaface). Therefore, the deep models trained with these databases can not be directly used under some specific scenes due to data bias. Re-collecting massive labeled data to train a new model from scratch or re-collecting some unlabeled data to perform domain adaptation [174] or others are effective methods.

Several popular benchmarks, such as LFW unrestricted protocol, Megaface Challenge 1, MS-Celeb-1M Challenge 1&2, explicitly encourage researchers to collect and clean a large-scale data set for enhancing deep neural network capability. Although data engineering is a valuable problem to computer vision researchers, this protocol is more incline to the in-

TABLE VI
THE COMMONLY USED FR DATASETS FOR TRAINING

Datasets	Publish Time	#photos	#subjects	# of photos per subject ¹	Key Features
MS-Celeb-1M (Challenge 1)[59]	2016	10M 3.8M(clean)	100,000 85K(clean)	100	breadth; central part of long tail; celebrity; knowledge base
MS-Celeb-1M (Challenge 2)[59]	2016	1.5M(base set) 1K(novel set)	20K(base set) 1K(novel set)	1/-/100	low-shot learning; tailed data; celebrity
MS-Celeb-1M (Challenge 3) [2]	2018	4M(MSV1c) 2.8M(Asian-Celeb)	80K(MSV1c) 100K(Asian-Celeb)	-	breadth;central part of long tail; celebrity
MegaFace [89], [119]	2016	4.7M	672,057	3/7/2469	breadth; the whole long tail;commonalty
VGGFace2 [20]	2017	3.31M	9,131	87/362.6/843	depth; head part of long tail; cross pose, age and ethnicity; celebrity
CASIA WebFace [206]	2014	494,414	10,575	2/46.8/804	celebrity
UMDFaces-Videos [9]	2017	22,075	3,107	-	video
VGGFace [123]	2015	2.6M	2,622	1,000	depth; celebrity; annotation with bounding boxesand coarse pose
CelebFaces+ [152]	2014	202,599	10,177	19.9	private
Google [144]	2015	>500M	>10M	50	private
Facebook [160]	2014	4.4M	4K	800/1100/1200	private

¹ The min/average/max numbers of photos or frames per subject

dustry participants. As evidence, the leaderboards of these experiments are mostly occupied by the companies holding invincible hardwares and data scales. This phenomenon may not be beneficial for developments of new model in academic community.

Owing to the source of data and cleaning strategies, existing large-scale datasets invariably contain label noises. Wang et al. [169] profiled the noise distribution in existing datasets in Fig. 17 and showed that the noise percentage increases dramatically along the scale of data. Moreover, they found that noise is more lethal on a 10,000-class problem of FR than on a 10-class problem of object classification and that label flip noise severely deteriorates the performance of a model, especially the model using A-softmax. Therefore, building a sufficiently large and cleaned dataset for academic research is very meaningful. Deng et al. [38] found there are sever label noise in MS-Celeb-1M, and they decreases the noise of MS-Celeb-1M, and makes the refined dataset public available. Microsoft and Deepglint jointly release the largest public data set with cleaned labels, which includes 4M images cleaned from MS-Celeb-1M dataset and 2.8M aligned images of 100K Asian celebrities. Moreover, Zhan et. al [216] shifted the focus from obtaining more manually labels to leveraging more unlabeled data. Through automatically assigning pseudo labels to unlabeled data with the help of relational graphs, they obtain competitive or even better results over the fully-supervised counterpart.

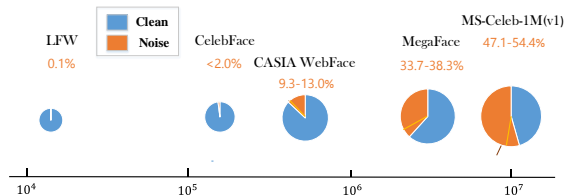


Fig. 17. A visualization of size and estimated noise percentage of datasets. [169]

B. Training protocols

In terms of training protocol, FR model can be evaluated under subject-dependent or independent settings, as illustrated in Fig. 18. For subject-dependent protocol, all testing identities are predefined in training set, it is natural to classify testing face images to the given identities. Therefore, subject-dependent FR can be well addressed as a classification problem, where features are expected to be separable. The protocol is mostly adopted by the early-stage (before 2010) FR studies on FERET [127], AR [113], and suitable only for some small-scale applications. MS-Celeb-1M is the only large-scale database using subject-dependent training protocol.

For subject-independent protocol, the testing identities are usually disjoint from the training set, which makes FR more challenging yet close to practice. Because it is impossible to classify faces to known identities in training set, subject-independent (generalized) representation is essential. Due to the fact that human faces exhibit similar intra-subject variations, deep models can display transcendental generalization ability when training with a sufficiently large set of generic subjects, where the key is to learn discriminative large-margin deep features. Almost all major face-recognition benchmarks, such as LFW, PaSC [14], IJB-A/B/C and Megaface, require the tested models to be trained under subject-independent protocol.

C. Evaluation tasks and performance metrics

In order to evaluate whether our deep models can solve the different problems of FR in real life, many testing datasets with different tasks and scenes are designed, which are listed in Table X. In terms of testing tasks, the performance of recognition model can be evaluated under face verification, close-set face identification, open-set face identification settings, as shown in Fig. 18. Each tasks have corresponding performance metrics.

Face verification is relevant to access control systems, re-identification, and application independent evaluations of FR algorithms. It is classically measured using the receiver

TABLE VII
PERFORMANCE OF STATE OF THE ARTS ON MEGAFACE DATASET

Method	Megaface challenge1				method	Megaface challenge2			
	FaceScrub		FGNet			FaceScrub		FGNet	
	Rank1 @10 ⁶	TPR @10 ⁻⁶ FPR	Rank1 @10 ⁶	TPR @10 ⁻⁶ FPR		Rank1 @10 ⁶	TPR @10 ⁻⁶ FPR	Rank1 @10 ⁶	TPR @10 ⁻⁶ FPR
Arcface [38]	0.9836	0.9848	-	-	Cosface [170]	0.7707	0.9030	0.6118	0.6350
Cosface [170]	0.9833	0.9841	-	-					
A-softmax [106]	0.9743	0.9766	-	-					
Marginal loss [39]	0.8028	0.9264	0.6643	0.4370					

TABLE VIII
PERFORMANCE OF STATE OF THE ARTS ON MS-CELEB-1M DATASET

Method	MS-celeb-1M challenge1			method	MS-celeb-1M challenge2		
	External Data	C@P=0.95 random set	C@P=0.95 hard set		External Data	Top 1 Accuracy base set	C@P=0.99 novel set
MCSM [196]	w	0.8750	0.7910	Cheng et al. [30]	w	0.9974	0.9901
Wang et al. [166]	w/o	0.7500	0.6060	Ding et al. [236]	w/o	-	0.9484
				Hybrid Classifiers [190]	w/o	0.9959	0.9264
				UP loss [58]	w/o	0.9980	0.7748

TABLE IX
FACE IDENTIFICATION AND VERIFICATION EVALUATION OF STATE OF THE ARTS ON IJB-A DATASET

Method	IJB-A Verification (TAR@FAR)			IJB-A Identification			
	0.001	0.01	0.1	FPIR=0.01	FPIR=0.1	Rank=1	Rank=10
L2-softmax [129]	0.943±0.005	0.970±0.004	0.984±0.002	0.915±0.041	0.956±0.006	0.973±0.005	0.988±0.003
DA-GAN [230]	0.930±0.005	0.976±0.007	0.991±0.003	0.890±0.039	0.949±0.009	0.971±0.007	0.989±0.003
VGGface2 [20]	0.921±0.014	0.968±0.006	0.990±0.002	0.883±0.038	0.946±0.004	0.982±0.004	0.994±0.001
TDFF [195]	0.919±0.006	0.961±0.007	0.988±0.003	0.878±0.035	0.941±0.010	0.964±0.006	0.992±0.002
NAN [204]	0.881±0.011	0.941±0.008	0.979±0.004	0.817±0.041	0.917±0.009	0.958±0.005	0.986±0.003
All-In-One Face [131]	0.823±0.02	0.922±0.01	0.976±0.004	0.792±0.02	0.887±0.014	0.947±0.008	0.988±0.003
Template Adaptation [36]	0.836±0.027	0.939±0.013	0.979±0.004	0.774±0.049	0.882±0.016	0.928±0.01	0.986±0.003
TPE [139]	0.813±0.02	0.90±0.01	0.964±0.005	0.753±0.03	0.863±0.014	0.932±0.01	0.977±0.005

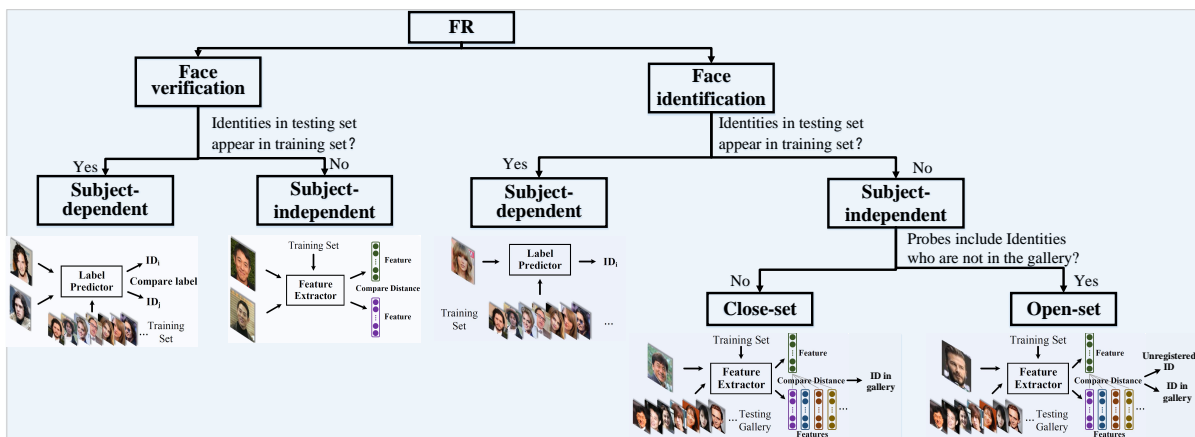


Fig. 18. The comparison of different training protocol and evaluation tasks. In terms of training protocol, FR model can be evaluated under subject-dependent or independent settings according to whether testing identities appear in training set. In terms of testing tasks, the performance of recognition model can be evaluated under face verification, close-set face identification, open-set face identification settings.

TABLE X
THE COMMONLY USED FR DATASETS FOR TESTING

Datasets	Publish Time	#photos	#subjects	# of photos per subject ¹	Metrics	Typical Methods & Accuracy ²	Key Features (Section)
LFW [77]	2007	13K	5K	1/2.3/530	1:1: Acc, TAR vs. FAR (ROC); 1:N: Rank-N, DIR vs. FAR (CMC)	99.78% Acc [129]; 99.63% Acc [144]	annotation with several attribute
MS-Celeb-1M Challenge 1 [59]	2016	2K	1K	2	Coverage@P=0.95	random set: 87.50%@P=0.95 hard set: 79.10%@P=0.95 [197] ¹	large-scale
MS-Celeb-1M Challenge 2 [59]	2016	100K(base set) 20K(novel set)	20K(base set) 1K(novel set)	5/-/20	Coverage@P=0.99	99.01%@P=0.99 [30]	low-shot learning (VI-C1)
MS-Celeb-1M Challenge 3 [2]	2018	274K(ELFW) 1M(DELFV)	5.7K(ELFW) 1.58M(DELFV)	-	1:1: TPR@FPR=1e-9; 1:N: TPR@FPR=1e-3	1:1: 46.15% [38] 43.88% [38]	trillion pairs; large distractors
MegaFace [89], [119]	2016	1M	690,572	1.4	1:1: TPR vs. FPR (ROC); 1:N: Rank-N (CMC)	1:1: 86.47%@10 ⁻⁶ FPR [144]; 1:N: 70.50% Rank-1 [144]	large-scale; 1 million distractors
IJB-A [93]	2015	25,809	500	11.4	1:1: TAR vs. FAR (ROC); 1:N: Rank-N, TPIR vs. FPPIR (CMC, DET)	1:1: 92.10%@10 ⁻³ FAR [20]; 1:N: 98.20% Rank-1 [20]	cross-pose; template-based (VI-A1 and VI-C2)
IJB-B [182]	2017	11,754 images 7,011 videos	1,845	36.2	1:1: TAR vs. FAR (ROC); 1:N: Rank-N, TPIR vs. FPPIR (CMC, DET)	1:1: 70.50%@10 ⁻⁵ FAR [20]; 1:N: 90.20% Rank-1 [20]	cross-pose; template-based (VI-A1 and VI-C2)
CPLFW [232]	2017	11652	3968	2/2.9/3	1:1: Acc, TAR vs. FAR (ROC)	77.90% Acc [123]	cross-pose (VI-A1)
CFP [145]	2016	7,000	500	14	1:1: Acc, EER, AUC, TAR vs. FAR (ROC)	Frontal-Frontal: 98.67% Acc [125]; Frontal-Profile: 94.39% Acc [211]	frontal-profile (VI-A1)
SLLFW [45]	2017	13K	5K	2.3	1:1: Acc, TAR vs. FAR (ROC)	85.78% Acc [123]; 78.78% Acc [160]	fine-grained
UMDFaces [10]	2016	367,920	8,501	43.3	1:1: Acc, TPR vs. FPR (ROC)	69.30%@10 ⁻² FAR [94]	annotation with bounding boxes, 21 keypoints, gender and 3D pose
YTF [183]	2011	3,425	1,595	48/181.3/6,070	1:1: Acc	97.30% Acc [123]; 96.52% Acc [133]	video (VI-C3)
PaSC [14]	2013	2,802	265	-	1:1: VR vs. FAR (ROC)	95.67%@10 ⁻² FAR [133]	video (VI-C3)
YTC [91]	2008	1,910	47	-	1:N: Rank-N (CMC)	97.82% Rank-1 [133]; 97.32% Rank-1 [132]	video (VI-C3)
CALFW [234]	2017	12174	4025	2/3/4	1:1: Acc, TAR vs. FAR (ROC)	86.50% Acc [123]; 82.52% Acc [23]	cross-age; 12 to 81 years old (VI-A2)
MORPH [135]	2006	55,134	13,618	4.1	1:N: Rank-N (CMC)	94.4% Rank-1 [102]	cross-age, 16 to 77 years old (VI-A2)
CACD [24]	2014	163,446	2000	81.7	1:1 (CACD-VS): Acc, TAR vs. FAR (ROC) 1:N: MAP	1:1 (CACD-VS): 98.50% Acc [180] 1:N: 69.96% MAP (2004-2006)[233]	cross-age, 14 to 62 years old (VI-A2)
FG-NET [1]	2010	1,002	82	12.2	1:N: Rank-N (CMC)	88.1% Rank-1 [180]	cross-age, 0 to 69 years old (VI-A2)
CASIA NIR-VIS v2.0 [98]	2013	17,580	725	24.2	1:1: Acc, VR vs. FAR (ROC)	98.62% Acc, 98.32%@10 ⁻³ FAR [189]	NIR-VIS; with eyeglasses, pose and expression variation (VI-B1)
CASIA-HFB [9]	2009	5097	202	25.5	1:1: Acc, VR vs. FAR (ROC)	97.58% Acc, 85.00%@10 ⁻³ FAR [134]	NIR-VIS; with eyeglasses and expression variation (VI-B1)
CUFS [176]	2009	1,212	606	2	1:N: Rank-N (CMC)	100% Rank-1 [220]	sketch-photo (VI-B3)
CUFSS [223]	2011	2,388	1,194	2	1:N: Rank-N (CMC)	51.00% Rank-1 [173]	sketch-photo; lighting variation; shape exaggeration (VI-B3)
Bosphorus [141]	2008	4,652	105	31/44.3/54	1:1: TAR vs. FAR (ROC); 1:N: Rank-N (CMC)	1:N: 99.20% Rank-1 [90]	3D; 34 expressions, 4 occlusions and different poses (VI-D1)
BU-3DPE [210]	2006	2,500	100	25	1:1: TAR vs. FAR (ROC); 1:N: Rank-N (CMC)	1:N: 95.00% Rank-1 [90]	3D; different expressions (VI-D1)
FRGCv2 [126]	2005	4,007	466	1/8/6/22	1:1: TAR vs. FAR (ROC); 1:N: Rank-N (CMC)	1:N: 94.80% Rank-1 [90]	3D; different expressions (VI-D1)
Guo et al. [55]	2014	1,002	501	2	1:1: Acc, TAR vs. FAR (ROC)	94.8% Rank-1, 65.9%@10 ⁻³ FAR [100]	make-up; female (VI-A3)
FAM [74]	2013	1,038	519	2	1:1: Acc, TAR vs. FAR (ROC)	88.1% Rank-1, 52.6%@10 ⁻³ FAR [100]	make-up; female and male (VI-A3)
CASIA-FASD [228]	2012	600	50	12	EER, HTER	2.67% EER, 2.27% HTER [8]	anti-spoofing (VI-D3)
Replay-Attack [31]	2012	1,300	50	-	EER, HTER	0.79% EER, 0.72% HTER [8]	anti-spoofing (VI-D3)

¹ The min/average/max numbers of photos or frames per subject

² We only present the typical methods that are published in a paper, and the accuracies of the most challenging scenarios are given.

operating characteristic (ROC) and estimated mean accuracy (ACC). At a given threshold (the independent variable), ROC analysis measures the true accept rate (TAR), which is the fraction of genuine comparisons that correctly exceed the threshold, and the false accept rate (FAR), which is the fraction of impostor comparisons that incorrectly exceed the threshold. And ACC is a simplified metric introduced by LFW, which represents the percentage of correct classifications. With the development of deep FR, the degree of security is required more and more strictly by testing datasets in order to match the fact that customers concern more about the TAR when FAR is kept in a very low rate in most security certification scenario. PaSC evaluates the TAR at a FAR of 10^{-2} ; IJB-A increases it to TAR@ 10^{-3} FAR; Megaface focuses on TAR@ 10^{-6} FAR; especially, in MS-celeb-1M challenge 3, TAR@ 10^{-9} FAR is required.

Close-set face identification is relevant to user driven searches (e.g., forensic identification), rank-N and cumulative match characteristic (CMC) is commonly used metrics in this scenario. Rank-N is based on what percentage of probe searches return the probe's gallery mate within the top k rank-ordered results. The CMC curve reports the percentage of probes identified within a given rank (the independent variable). IJB-A/B/C concern on the rank-1 and rank-5 recognition rate. The MegaFace challenge systematically evaluates rank-1 recognition rate function of increasing number of gallery distractors (going from 10 to 1 Million), the evaluation of state of the arts are listed in Table VII. Rather than rank-N and CMC, MS-Celeb-1M further applies a precision-coverage curve to measure identification performance under a variable threshold t . The probe is rejected when its confidence score is lower than t . The algorithms are compared in term of what fraction of passed probes, i.e. coverage, with a high recognition precision, e.g. 95% or 99%, the evaluation of state of the arts are listed in Table VIII.

Open-set face identification is relevant to high throughput face search systems (e.g., de-duplication, watch list identification), where the recognition system should reject unknown/unseen subjects (probes who do not present in gallery) at test time. At present, there are very few databases covering the task of open-set FR. IJB-A benchmark introduces a decision error tradeoff (DET) curve to characterize the FNIR as function of FPIR. The false positive identification rate (FPIR) measures what fraction of comparisons between probe templates and non-mate gallery templates result in a match score exceeding T . At the same time, the false negative identification rate (FNIR) measures what fraction of probe searches will fail to match a mated gallery template above a score of T . The algorithms are compared in term of the FNIR at a low FPIR, e.g. 1% or 10%, the evaluation of state of the arts on IJB-A dataset as listed in Table IX.

D. Evaluation Scenes and Data

There are also many testing datasets with different scenes to mimic FR in real life as shown in Table X. According to their characteristics, we divide these scenes into four categories: cross-factor FR, heterogenous FR, multiple (or single) media FR and FR in industry (Fig. 19).

- **Cross-factor FR.** Due to the complex nonlinear facial appearance, some variations will be caused by people themselves, such as cross-pose, cross-age, make-up. For example, CALFW [234], MORPH [135], CACD [24] and FG-NET [1] are commonly used datasets with different age range; CFP [145] only focuses on frontal and profile face, CPLFW [232] is extended from LFW with different poses.
- **Heterogenous FR.** It refers to the problem of matching faces across different visual domains. The domain gap is mainly caused by sensory devices and cameras settings, e.g. visual light vs. near-infrared and photo vs. sketch. For example, as photo-sketch datasets, CUFSF [223] is harder than CUFS [176] due to lighting variation and shape exaggeration.
- **Multiple (or single) media FR.** Ideally, deep models are trained with massive images per person and are tested with one image per person, but the situation will be different in reality. Sometimes, the number of images per person in training set could be very small, namely low-shot FR, such as MS-Celeb-1M challenge 2; or each subject face in test set is often enrolled with a set of images and videos, namely set-based FR, such as IJB-A and PaSC.
- **FR in industry.** Although deep FR has achieved beyond human performance on some standard benchmarks, but some factors should be given more attention rather than accuracy when deep FR are adopted in industry, e.g. anti-spoofing (CASIA-FASD [228]) and 3D FR (Bosphorus [141], BU-3DFE [210] and FRGCv2 [126]). Compared to publicly available 2D face databases, 3D scans are hard to acquire, and the number of scans and subjects in public 3D face databases is still limited, which hinders the development of 3D deep FR.

VI. DIVERSE RECOGNITION SCENES

In order to do well in testing dataset with different scenes which are described in the last chapter, deep models need larger training datasets and excellent algorithm. However, public available training databases are mostly collected from the photos of celebrities due to privacy issue, it is far from images captured in the daily life with diverse scenes. Despite the high accuracy in the LFW, Megaface benchmarks, its performance still hardly meets the requirements in real-world application. A conjecture in industry is made that results of generic deep models can be improved simply by collecting big datasets of the target scene. However, this holds only to a certain degree. Therefore, significant efforts have been paid to address these scenes by excellent algorithms with very limited data. In this section, we present several special algorithms of FR under different scenes.

A. Cross-Factor Face Recognition

1) *Cross-Pose Face Recognition:* As [145] shows that many existing algorithms suffer a decrease of over 10% from frontal-frontal to frontal-profile verification, cross-pose FR is still

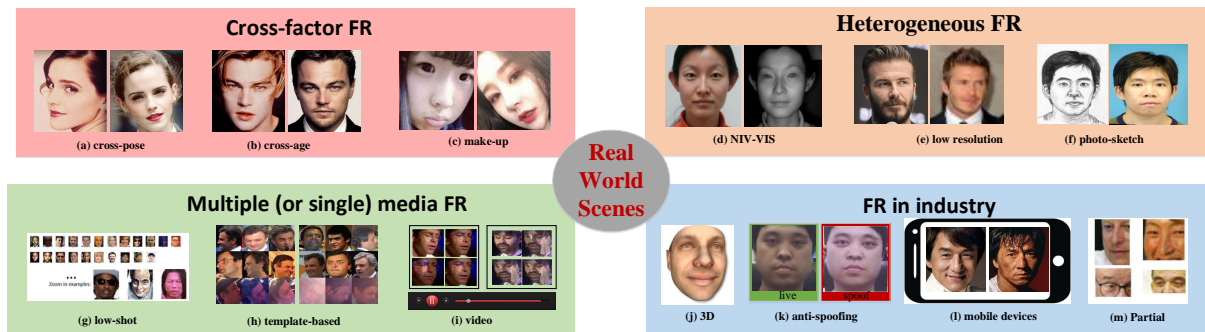


Fig. 19. The different scenes of FR. We divide FR scenes into four categories: cross-factor FR, heterogenous FR, multiple (or single) media FR and FR in industry. There are many testing datasets and special FR methods for each scene.

an extremely challenging scene. In addition to the aforementioned methods, including “one-to-many augmentation”, “many-to-one normalization”, multi-input networks and multi-task learning (Sections IV and III-B2), there are still some other algorithms for cross-pose FR. Considering the extra burden of the above methods, [19] first attempt to perform frontalization in the deep feature space but not in the image space. A deep residual equivariant mapping (DREAM) block dynamically adds residuals to an input representation to transform a profile face to a frontal image. [27] proposed combining feature extraction with multi-view subspace learning to simultaneously make poses more robust and discriminative. Pose Invariant Model (PIM) [83] jointly learn face frontalization and pose invariant representations end-to-end to allow them to mutually boost each other, and further introduced unsupervised cross-domain adversarial training and a learning to learn strategy to provide high-fidelity frontal reference face images.

2) *Cross-Age Face Recognition*: Cross-age FR is extremely challenging due to the changes in facial appearance by the aging process over time. One direct approach is to synthesize the input image to the target age. A generative probabilistic model was used by [49] to model the facial aging process at each short-term stage. The identity-preserved conditional generative adversarial networks (IPCGANs) [246] framework utilized a conditional-GAN to generate a face in which an identity-preserved module preserved the identity information and an age classifier forced the generated face with the target age. Antipov et al. [7] proposed aging faces by GAN, but the synthetic faces cannot be directly used for face verification due to its imperfect preservation of identities. Then, [6] used a local manifold adaptation (LMA) approach to solve the problem of [7]. In [200], high-level age-specific features conveyed by the synthesized face are estimated by a pyramidal adversarial discriminator at multiple scales to generate more lifelike facial details. An alternative is to decompose aging/identity components separately and extract age-invariant representations. Wen et. al [180] developed a latent identity analysis (LIA) layer to separate the two components (Fig. 20). In [233], age-invariant features were obtained by subtracting age-specific factors from the representations with the help of the age estimation task. In [169], face features are decomposed in the spherical coordinate system, the identity-related components are represented with

angular coordinates and the age-related information is encoded with radial coordinate. Additionally, there are other methods for cross-age FR. For example, [15], [50] fine-tuned the CNN to transfer knowledge. Wang et al. [177] proposed a siamese deep network of multi-task learning of FR and age estimation. Li et al. [101] integrated feature extraction and metric learning via a deep CNN.

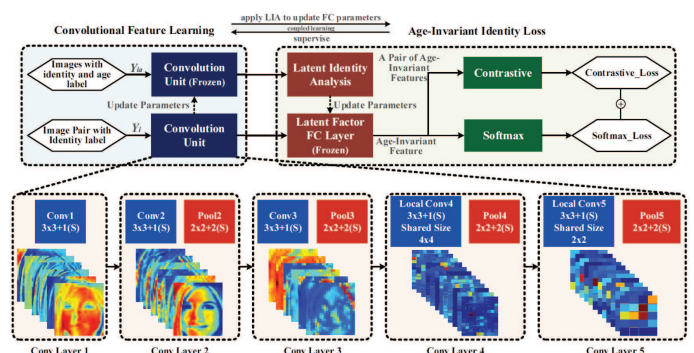


Fig. 20. The architecture of the cross-age FR with LIA. [180]

3) *Makeup Face Recognition*: Makeup is widely used by the public today, but it also brings challenges for FR due to significant facial appearance changes. The research on matching makeup and nonmakeup face images is receiving increasing attention. Li et. al [100] generated nonmakeup images from makeup ones by a bi-level adversarial network (BLAN) and then used the synthesized nonmakeup images for verification (Fig. 21). Sun et. al [154] pretrained a triplet network on the free videos and fine-tuned it on small makeup and nonmakeup datasets.

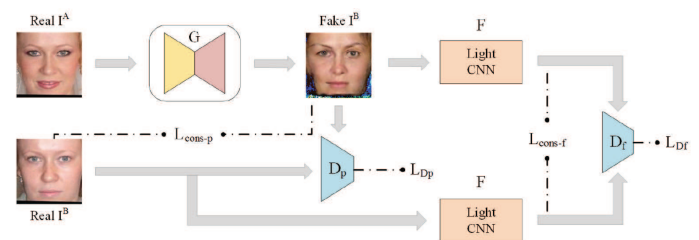


Fig. 21. The architecture of BLAN. [100]

B. Heterogenous Face Recognition

1) *NIR-VIS Face Recognition*: Due to the excellent performance of the near-infrared spectrum (NIS) images under low-light scenarios, NIS images are widely applied in surveillance systems. Because most enrolled databases consist of visible light (VIS) spectrum images, how to recognize a NIR face from a gallery of VIS images has been a hot topic. [142], [109] transferred the VIS deep networks to the NIR domain by fine-tuning. Lezama et. al [96] used a VIS CNN to recognize NIR faces by transforming NIR images to VIS faces through cross-spectral hallucination and restoring a low-rank structure for features through low-rank embedding. Reale et. al [134] trained two networks, a VISNet (for visible images) and a NIRNet (for near-infrared images), and coupled their output features by creating a siamese network. [68], [69] divided the high layer of the network into a NIR layer, a VIS layer and a NIR-VIS shared layer; then, a modality-invariant feature can be learned by the NIR-VIS shared layer. Song et. al [151] embedded cross-spectral face hallucination and discriminative feature learning into an end-to-end adversarial network. In [189], the low-rank relevance and cross-modal ranking were used to alleviate the semantic gap.

2) *Low-Resolution Face Recognition*: Although deep networks are robust to a degree of low resolution, there are still a few studies focused on promoting the performance of low-resolution FR. For example, Zangeneh et. al [215] proposed a CNN with a two-branch architecture (a super-resolution network and a feature extraction network) to map the high- and low-resolution face images into a common space where the intra-person distance is smaller than the inter-person distance. Shen et. al [245] exploited the face semantic information as global priors and local structural constraints to better restore the shape and detail of face images. In addition, they optimized the network with perceptual and adversarial losses to produce photo-realistic results.

3) *Photo-Sketch Face Recognition*: The photo-sketch FR may help law enforcement to quickly identify suspects. The commonly used methods can be categorized as two classes. One is to utilize transfer learning to directly match photos to sketches, where the deep networks are first trained using a large face database of photos and are then fine-tuned using small sketch database [117], [51]. The other is to use the image-to-image translation, where the photo can be transformed to a sketch or the sketch to a photo; then, FR can be performed in one domain. [220] developed a fully convolutional network with generative loss and a discriminative regularizer to transform photos to sketches. Zhang et. al [218] utilized a branched fully convolutional neural network (BFCN) to generate a structure-preserved sketch and a texture-preserved sketch, and then they fused them together via a probabilistic method. Recently, GANs have achieved impressive results in image generation. [207], [92], [240] used two generators, G_A and G_B , to generate sketches from photos and photos from sketches, respectively (Fig. 22). Based on [240], Wang et. al [173] proposed a multi-adversarial network to avoid artifacts by leveraging the implicit presence of feature maps of different resolutions in the generator subnetwork.

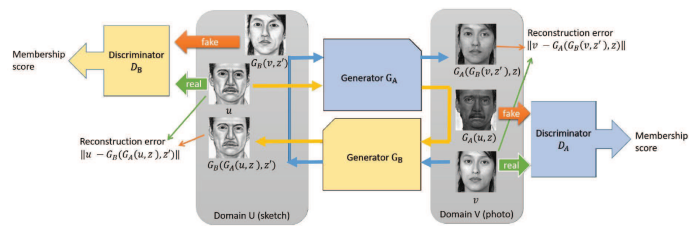


Fig. 22. The architecture of DualGAN. [207]

C. Multiple (or single) media Face Recognition

1) *Low-Shot Face Recognition*: For many practical applications, such as surveillance and security, the FR system should recognize persons with a very limited number of training samples or even with only one sample. The methods of low-shot learning can be categorized as enlarging the training data and learning more powerful features. Hong et. al [71] generated images in various poses using a 3D face model and adopted deep domain adaptation to handle the other variations, such as blur, occlusion, and expression (Fig. 23). Choe et. al [32] used data augmentation methods and a GAN for pose transition and attribute boosting to increase the size of the training dataset. Wu et. al [190] proposed a framework with hybrid classifiers using a CNN and a nearest neighbor (NN) model. Guo et. al [58] made the norms of the weight vectors of the one-shot classes and the normal classes aligned to address the data imbalance problem. Cheng et. al [30] proposed an enforced softmax that contains optimal dropout, selective attenuation, L2 normalization and model-level optimization. Yin et al. [213] augmented feature space of low-shot classes by transferring the principal components from regular to low-shot classes to encourage the variance of low-shot classes to mimic that of regular classes.

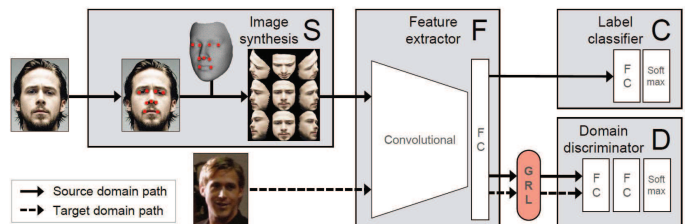


Fig. 23. The architecture of a single sample per person domain adaptation network (SSPP-DAN). [71]

2) *Set/Template-Based Face Recognition*: Set/template-based FR problems assume that both probe and gallery sets are represented using a set of media, e.g., images and videos, rather than just one. After learning a set of face representations from each medium individually, two strategies are generally adopted for face recognition between sets. One is to use these representations for similarity comparison between the media in two sets and pool the results into a single, final score, such as max score pooling [115], average score pooling [112] and its variations [229], [17]. The other strategy is to aggregate face representations through average or max pooling and generate a single representation for each set and then perform a comparison between two sets, which we

call feature pooling [115], [28], [139]. In addition to the commonly used strategies, there are also some novel methods proposed for set/template-based FR. For example, Hayat et. al [63] proposed a deep heterogeneous feature fusion network to exploit the features' complementary information generated by different CNNs. Liu et. al [110] introduced the actor-critic reinforcement learning for set-based FR. They casted the inner-set dependency modeling to a Markov decision process in the latent space, and train an dependency-aware attention control agent to make attention control for each image in each step.

3) *Video Face Recognition*: There are two key issues in video FR: one is to integrate the information across different frames together to build a representation of the video face, and the other is to handle video frames with severe blur, pose variations, and occlusions. For frame aggregation, Yang et. al [204] proposed a neural aggregation network (NAN) in which the aggregation module, consisting of two attention blocks driven by a memory, produces a 128-dimensional vector representation (Fig. 24). Rao et al. [132] aggregated raw video frames directly by combining the idea of metric learning and adversarial learning. For handling bad frames, Rao et. al [133] discarded the bad frames by treating this operation as a Markov decision process and trained the attention model through a deep reinforcement learning framework. Ding et. al [47] artificially blurred clear still images for training to learn blur-robust face representations. Parchami et al. [121] used a CNN to reconstruct a lower-quality video into a high-quality face.

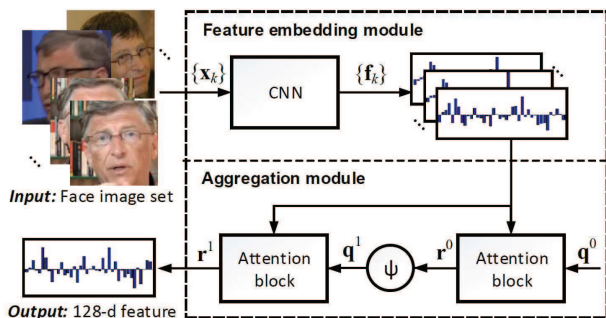


Fig. 24. The FR framework of NAN. [204]

D. Face Recognition in Industry

1) *3D Face Recognition*: 3D FR has inherent advantages over 2D methods, but 3D deep FR is not well developed due to the lack of large annotated 3D data. To enlarge 3D training datasets, most works use the methods of “one-to-many augmentation” to synthesize 3D faces. However, the effective methods for extracting deep features of 3D faces remain to be explored. Kim et. al [90] fine-tuned a 2D CNN with a small amount of 3D scans for 3D FR. Zulqarnain et. al [248] used a three-channel (corresponding to depth, azimuth and elevation angles of the normal vector) image as input and minimized the average prediction log-loss. Zhang et. al [219] selected 30 feature points from the Candide-3 face model to characterize

faces and then conducted the unsupervised pretraining of face depth data and the supervised fine-tuning.

2) *Partial Face Recognition*: Partial FR, in which only arbitrary-size face patches are presented, has become an emerging problem with increasing requirements of identification from CCTV cameras and embedded vision systems in mobile devices, robots and smart home facilities. He et. al [67] divided the aligned face image into several multi-scale patches and the dissimilarity between two partial face images is calculated as the weighted l_2 distance between corresponding patches. Dynamic feature matching (DFM) [66] utilized a sliding window of the same size as the probe feature maps to decompose the gallery feature maps into several gallery sub-feature maps, and the similarity-guided constraint imposed on sparse representation classification (SRC) provides an alignment-free matching.

3) *Face Anti-spoofing*: With the success of FR techniques, various types of spoofing attacks, such as print attacks, replay attacks, and 3D mask attacks, are becoming a large threat. Face anti-spoofing is a very critical step to recognize whether the face is live or spoofed. Because it also needs to recognize faces (true or false identity), we treat it as one of the FR scenes. Atoum et. al [8] proposed a novel two-stream CNN in which the local features discriminate the spoof patches independent of the spatial face areas, and holistic depth maps ensure that the input live sample has a face-like depth. Yang et. al [202] trained a CNN using both a single frame and multiple frames with five scales as input, and the live/spoof label is assigned as the output. Xu et. al [198] proposed a long short-term memory (LSTM)-CNN architecture that learns temporal features to jointly predict for multiple frames of a video. [97], [124] fine-tuned their networks from a pretrained model by training sets of real and fake images. Jourabloo et. al [84] proposed to inversely decompose a spoof face into the live face and the spoof noise pattern. They designed loss functions to encourage the pattern of the spoof images to be ubiquitous and repetitive, while the noise of the live images should be zero.

4) *Face Recognition for Mobile Devices*: With the emergence of mobile phones, tablets and augmented reality, FR has been applied in mobile devices. Due to computational limitations, the recognition tasks in these devices need to be carried out in a light but timely fashion. As mentioned in Section III-B1, [79], [72], [33], [226] proposed lightweight deep networks, and these networks have potential to be introduced into FR. [159] proposed a minibatch method that first generates signatures for a minibatch of k face images and then constructs an unbiased estimate of the full gradient by relying on all $k^2 - k$ pairs from the minibatch.

VII. CONCLUSIONS

In this paper, we provide a comprehensive survey of deep FR from two aspects of data and algorithms. For algorithms, some mainstream and special network architectures are presented. Meanwhile, we categorize loss functions into Euclidean-distance-based loss, angular/cosine-margin-based loss and softmax loss and its variations. For data, we

summarize some commonly used FR datasets. Moreover, the methods of face processing are introduced and categorized as “one-to-many augmentation” and “many-to-one normalization”. Finally, the different scenes of deep FR, including video FR, 3D FR and cross-age FR, are briefly introduced.

Thanks to the massive amounts of annotated data, algorithms and GPUs, deep FR has achieved beyond human performance on some standard benchmarks on near-frontal face verification, similar-looking face discrimination, and cross-age face verification. However, comprehensive abilities are required before large-scale applications, and many issues still remain to be addressed, as follows:

- Because real-world FR is much more complex and strict than in the experiments, the FR system is still far from human performance in real-world settings. Improving the true positive rate while keeping a very low false positive rate is crucial; handling data bias and variations needs continued attention.
- Corresponding to three datasets, namely, MegaFace, MS-Celeb-1M and IJB-A, large-scale FR with a very large number of candidates, low/one-shot FR and large pose-variance FR will be the focus of research in the future.
- Face recognition can be inspired from human behaviors. For examples, for humans, familiar faces are recognized more accurately than unfamiliar ones and under difficult viewing conditions. Developing a deep model to encode face familiarity is important to FR under extreme conditions and open-set scenarios. Moreover, humans can complete the recognition task in one step, so there is a bright prospect in the joint alignment-representation networks.
- The first layer of deep networks can be viewed directly by visualization and is found to be similar to a Gabor filter, which realizes the edge detection. However, our understanding of how the whole deep networks operate, particularly what computations they perform at higher layers, has lagged behind. It is undoubtedly of great significance for the development of deep FR to open the black box and study the effective interpretation of high-level features.
- There are still many challenges in adopting deep FR in industry. Although face anti-spoofing has achieved successes in resisting print, replay, and 3D mask attacks, a new type of misclassification attack via physically realizable attack artifacts [147], [146] causes a rising interest, proving that FR systems are still not robust and are vulnerable to attacks. Meanwhile, the recognition tasks in mobile devices need to be carried out in a light but timely fashion. Therefore, improving the defensiveness of systems and the efficiency of computing are to be solved.
- Other challenges are included in our lists of deep FR scenes. When facing these different scenes in real-world settings, the system should make specific adjustments accordingly. How to work out a more general system or a system that can be applied in every scene after little modification may be the direction in the future. Deep

domain adaptation [174] has inherent advantages here and is worthy of attention.

REFERENCES

- [1] Fg-net aging database. <http://www.fgnet.rsunit.com>.
- [2] Ms-celeb-1m challenge 3. <http://trillionpairs.deeplint.com>.
- [3] A. F. Abate, M. Nappi, D. Riccio, and G. Sabatino. 2d and 3d face recognition: A survey. *Pattern recognition letters*, 28(14):1885–1906, 2007.
- [4] W. Abdalmageed, Y. Wu, S. Rawls, S. Harel, T. Hassner, I. Masi, J. Choi, J. Lekust, J. Kim, and P. Natarajan. Face recognition using deep multi-pose representations. In *WACV*, pages 1–9, 2016.
- [5] T. Ahonen, A. Hadid, and M. Pietikainen. Face description with local binary patterns: Application to face recognition. *IEEE Trans. Pattern Anal. Machine Intell.*, 28(12):2037–2041, 2006.
- [6] G. Antipov, M. Baccouche, and J.-L. Dugelay. Boosting cross-age face verification via generative age normalization. In *IJCB*, 2017.
- [7] G. Antipov, M. Baccouche, and J.-L. Dugelay. Face aging with conditional generative adversarial networks. *arXiv preprint arXiv:1702.01983*, 2017.
- [8] Y. Atoum, Y. Liu, A. Jourabloo, and X. Liu. Face anti-spoofing using patch and depth-based cnns. In *IJCB*, pages 319–328. IEEE, 2017.
- [9] A. Bansal, C. Castillo, R. Ranjan, and R. Chellappa. The dos and donts for cnn-based face verification. *arXiv preprint arXiv:1705.07426*, 5, 2017.
- [10] A. Bansal, A. Nanduri, C. Castillo, R. Ranjan, and R. Chellappa. Umdfaces: An annotated face dataset for training deep networks. *arXiv preprint arXiv:1611.01484*, 2016.
- [11] J. Bao, D. Chen, F. Wen, H. Li, and G. Hua. Cvae-gan: fine-grained image generation through asymmetric training. *arXiv preprint arXiv:1703.10155*, 2017.
- [12] J. Bao, D. Chen, F. Wen, H. Li, and G. Hua. Towards open-set identity preserving face synthesis. In *CVPR*, pages 6713–6722, 2018.
- [13] P. N. Belhumeur, J. P. Hespanha, and D. J. Kriegman. Eigenfaces vs. fisherfaces: Recognition using class specific linear projection. *IEEE Trans. Pattern Anal. Mach. Intell.*, 19(7):711–720, 1997.
- [14] J. R. Beveridge, P. J. Phillips, D. S. Bolme, B. A. Draper, G. H. Givens, Y. M. Lui, M. N. Teli, H. Zhang, W. T. Scruggs, K. W. Bowyer, et al. The challenge of face recognition from digital point-and-shoot cameras. In *BTAS*, pages 1–8. IEEE, 2013.
- [15] S. Bianco. Large age-gap face verification by feature injection in deep networks. *Pattern Recognition Letters*, 90:36–42, 2017.
- [16] V. Blanz and T. Vetter. Face recognition based on fitting a 3d morphable model. *IEEE Transactions on pattern analysis and machine intelligence*, 25(9):1063–1074, 2003.
- [17] N. Bodla, J. Zheng, H. Xu, J.-C. Chen, C. Castillo, and R. Chellappa. Deep heterogeneous feature fusion for template-based face recognition. In *WACV*, pages 586–595. IEEE, 2017.
- [18] K. W. Bowyer, K. Chang, and P. Flynn. A survey of approaches and challenges in 3d and multi-modal 3d+ 2d face recognition. *Computer vision and image understanding*, 101(1):1–15, 2006.
- [19] K. Cao, Y. Rong, C. Li, X. Tang, and C. C. Loy. Pose-robust face recognition via deep residual equivariant mapping. *arXiv preprint arXiv:1803.00839*, 2018.
- [20] Q. Cao, L. Shen, W. Xie, O. M. Parkhi, and A. Zisserman. Vggface2: A dataset for recognising faces across pose and age. *arXiv preprint arXiv:1710.08092*, 2017.
- [21] Z. Cao, Q. Yin, X. Tang, and J. Sun. Face recognition with learning-based descriptor. In *CVPR*, pages 2707–2714. IEEE, 2010.
- [22] T.-H. Chan, K. Jia, S. Gao, J. Lu, Z. Zeng, and Y. Ma. Pcanet: A simple deep learning baseline for image classification? *IEEE Transactions on Image Processing*, 24(12):5017–5032, 2015.
- [23] B. Chen, W. Deng, and J. Du. Noisy softmax: improving the generalization ability of dcnn via postponing the early softmax saturation. *arXiv preprint arXiv:1708.03769*, 2017.
- [24] B.-C. Chen, C.-S. Chen, and W. H. Hsu. Cross-age reference coding for age-invariant face recognition and retrieval. In *ECCV*, pages 768–783. Springer, 2014.
- [25] D. Chen, X. Cao, L. Wang, F. Wen, and J. Sun. Bayesian face revisited: A joint formulation. In *ECCV*, pages 566–579. Springer, 2012.
- [26] D. Chen, X. Cao, F. Wen, and J. Sun. Blessing of dimensionality: High-dimensional feature and its efficient compression for face verification. In *CVPR*, pages 3025–3032, 2013.
- [27] G. Chen, Y. Shao, C. Tang, Z. Jin, and J. Zhang. Deep transformation learning for face recognition in the unconstrained scene. *Machine Vision and Applications*, pages 1–11, 2018.
- [28] J.-C. Chen, V. M. Patel, and R. Chellappa. Unconstrained face verification using deep cnn features. In *WACV*, pages 1–9. IEEE, 2016.

- [29] J.-C. Chen, R. Ranjan, A. Kumar, C.-H. Chen, V. M. Patel, and R. Chellappa. An end-to-end system for unconstrained face verification with deep convolutional neural networks. In *ICCV Workshops*, pages 118–126, 2015.
- [30] Y. Cheng, J. Zhao, Z. Wang, Y. Xu, K. Jayashree, S. Shen, and J. Feng. Know you at one glance: A compact vector representation for low-shot learning. In *CVPR*, pages 1924–1932, 2017.
- [31] I. Chingovska, A. Anjos, and S. Marcel. On the effectiveness of local binary patterns in face anti-spoofing. 2012.
- [32] J. Choe, S. Park, K. Kim, J. H. Park, D. Kim, and H. Shim. Face generation for low-shot learning using generative adversarial networks. In *ICCV Workshops*, pages 1940–1948. IEEE, 2017.
- [33] F. Chollet. Xception: Deep learning with depthwise separable convolutions. *arXiv preprint*, 2016.
- [34] A. R. Chowdhury, T.-Y. Lin, S. Maji, and E. Learned-Miller. One-to-many face recognition with bilinear cnns. In *WACV*, pages 1–9. IEEE, 2016.
- [35] F. Cole, D. Belanger, D. Krishnan, A. Sarna, I. Mosseri, and W. T. Freeman. Synthesizing normalized faces from facial identity features. In *CVPR*, pages 3386–3395, 2017.
- [36] N. Crosswhite, J. Byrne, C. Stauffer, O. Parkhi, Q. Cao, and A. Zisserman. Template adaptation for face verification and identification. In *FG 2017*, pages 1–8, 2017.
- [37] J. Deng, S. Cheng, N. Xue, Y. Zhou, and S. Zafeiriou. Uv-gan: Adversarial facial uv map completion for pose-invariant face recognition. *arXiv preprint arXiv:1712.04695*, 2017.
- [38] J. Deng, J. Guo, and S. Zafeiriou. Arcface: Additive angular margin loss for deep face recognition. *arXiv preprint arXiv:1801.07698*, 2018.
- [39] J. Deng, Y. Zhou, and S. Zafeiriou. Marginal loss for deep face recognition. In *CVPR Workshops*, volume 4, 2017.
- [40] W. Deng, J. Hu, and J. Guo. Extended src: Undersampled face recognition via intraclass variant dictionary. *IEEE Trans. Pattern Anal. Machine Intell.*, 34(9):1864–1870, 2012.
- [41] W. Deng, J. Hu, and J. Guo. Compressive binary patterns: Designing a robust binary face descriptor with random-field eigenfilters. *IEEE Trans. Pattern Anal. Mach. Intell.*, PP(99):1–1, 2018.
- [42] W. Deng, J. Hu, and J. Guo. Face recognition via collaborative representation: Its discriminant nature and superposed representation. *IEEE Trans. Pattern Anal. Mach. Intell.*, PP(99):1–1, 2018.
- [43] W. Deng, J. Hu, J. Guo, H. Zhang, and C. Zhang. Comments on “globally maximizing, locally minimizing: Unsupervised discriminant projection with applications to face and palm biometrics”. *IEEE Trans. Pattern Anal. Mach. Intell.*, 30(8):1503–1504, 2008.
- [44] W. Deng, J. Hu, J. Lu, and J. Guo. Transform-invariant pca: A unified approach to fully automatic facealignment, representation, and recognition. *IEEE Trans. Pattern Anal. Mach. Intell.*, 36(6):1275–1284, June 2014.
- [45] W. Deng, J. Hu, N. Zhang, B. Chen, and J. Guo. Fine-grained face verification: Fglfw database, baselines, and human-dcmn partnership. *Pattern Recognition*, 66:63–73, 2017.
- [46] C. Ding and D. Tao. Robust face recognition via multimodal deep face representation. *IEEE Transactions on Multimedia*, 17(11):2049–2058, 2015.
- [47] C. Ding and D. Tao. Trunk-branch ensemble convolutional neural networks for video-based face recognition. *IEEE transactions on pattern analysis and machine intelligence*, 2017.
- [48] P. Dou, S. K. Shah, and I. A. Kakadiaris. End-to-end 3d face reconstruction with deep neural networks. In *CVPR*, volume 5, 2017.
- [49] C. N. Duong, K. G. Quach, K. Luu, M. Savvides, et al. Temporal non-volume preserving approach to facial age-progression and age-invariant face recognition. *arXiv preprint arXiv:1703.08617*, 2017.
- [50] H. El Khyari and H. Wechsler. Age invariant face recognition using convolutional neural networks and set distances. *Journal of Information Security*, 8(03):174, 2017.
- [51] C. Galea and R. A. Farrugia. Forensic face photo-sketch recognition using a deep learning-based architecture. *IEEE Signal Processing Letters*, 24(11):1586–1590, 2017.
- [52] M. M. Ghazi and H. K. Ekenel. A comprehensive analysis of deep learning based representation for face recognition. In *CVPR Workshops*, volume 26, pages 34–41, 2016.
- [53] I. Goodfellow, J. Pouget-Abadie, M. Mirza, B. Xu, D. Warde-Farley, S. Ozair, A. Courville, and Y. Bengio. Generative adversarial nets. In *NIPS*, pages 2672–2680, 2014.
- [54] P. J. Grother and L. N. Mei. Face recognition vendor test (frvt) performance of face identification algorithms nist ir 8009. *NIST Interagency/Internal Report (NISTIR) - 8009*, 2014.
- [55] G. Guo, L. Wen, and S. Yan. Face authentication with makeup changes. *IEEE Transactions on Circuits and Systems for Video Technology*, 24(5):814–825, 2014.
- [56] S. Guo, S. Chen, and Y. Li. Face recognition based on convolutional neural network and support vector machine. In *IEEE International Conference on Information and Automation*, pages 1787–1792, 2017.
- [57] Y. Guo, J. Zhang, J. Cai, B. Jiang, and J. Zheng. 3dfacenet: Real-time dense face reconstruction via synthesizing photo-realistic face images. 2017.
- [58] Y. Guo and L. Zhang. One-shot face recognition by promoting underrepresented classes. *arXiv preprint arXiv:1707.05574*, 2017.
- [59] Y. Guo, L. Zhang, Y. Hu, X. He, and J. Gao. Ms-celeb-1m: A dataset and benchmark for large-scale face recognition. In *ECCV*, pages 87–102. Springer, 2016.
- [60] C. Han, S. Shan, M. Kan, S. Wu, and X. Chen. Face recognition with contrastive convolution. In *The European Conference on Computer Vision (ECCV)*, September 2018.
- [61] A. Hasnat, J. Bohné, J. Milgram, S. Gentric, and L. Chen. Deepvisage: Making face recognition simple yet with powerful generalization skills. *arXiv preprint arXiv:1703.08388*, 2017.
- [62] M. Hasnat, J. Bohné, J. Milgram, S. Gentric, L. Chen, et al. von mises-fisher mixture model-based deep learning: Application to face verification. *arXiv preprint arXiv:1706.04264*, 2017.
- [63] M. Hayat, M. Bennamoun, and S. An. Learning non-linear reconstruction models for image set classification. In *CVPR*, pages 1907–1914, 2014.
- [64] M. Hayat, S. H. Khan, N. Werghi, and R. Goecke. Joint registration and representation learning for unconstrained face identification. In *CVPR*, pages 2767–2776, 2017.
- [65] K. He, X. Zhang, S. Ren, and J. Sun. Deep residual learning for image recognition. In *CVPR*, pages 770–778, 2016.
- [66] L. He, H. Li, Q. Zhang, and Z. Sun. Dynamic feature learning for partial face recognition. In *The IEEE Conference on Computer Vision and Pattern Recognition (CVPR)*, June 2018.
- [67] L. He, H. Li, Q. Zhang, Z. Sun, and Z. He. Multiscale representation for partial face recognition under near infrared illumination. In *IEEE International Conference on Biometrics Theory, Applications and Systems*, pages 1–7, 2016.
- [68] R. He, X. Wu, Z. Sun, and T. Tan. Learning invariant deep representation for nir-vis face recognition. In *AAAI*, volume 4, page 7, 2017.
- [69] R. He, X. Wu, Z. Sun, and T. Tan. Wasserstein cnn: Learning invariant features for nir-vis face recognition. *arXiv preprint arXiv:1708.02412*, 2017.
- [70] X. He, S. Yan, Y. Hu, P. Niyogi, and H.-J. Zhang. Face recognition using laplacianfaces. *IEEE Trans. Pattern Anal. Mach. Intell.*, 27(3):328–340, 2005.
- [71] S. Hong, W. Im, J. Ryu, and H. S. Yang. Spp-dan: Deep domain adaptation network for face recognition with single sample per person. *arXiv preprint arXiv:1702.04069*, 2017.
- [72] A. G. Howard, M. Zhu, B. Chen, D. Kalenichenko, W. Wang, T. Weyand, M. Andreetto, and H. Adam. Mobilenets: Efficient convolutional neural networks for mobile vision applications. *arXiv preprint arXiv:1704.04861*, 2017.
- [73] G. Hu, Y. Yang, D. Yi, J. Kittler, W. Christmas, S. Z. Li, and T. Hospedales. When face recognition meets with deep learning: an evaluation of convolutional neural networks for face recognition. In *ICCV workshops*, pages 142–150, 2015.
- [74] J. Hu, Y. Ge, J. Lu, and X. Feng. Makeup-robust face verification. In *ICASSP*, pages 2342–2346. IEEE, 2013.
- [75] J. Hu, L. Shen, and G. Sun. Squeeze-and-excitation networks. *arXiv preprint arXiv:1709.01507*, 2017.
- [76] L. Hu, M. Kan, S. Shan, X. Song, and X. Chen. Ldf-net: Learning a displacement field network for face recognition across pose. In *FG 2017*, pages 9–16. IEEE, 2017.
- [77] G. B. Huang, M. Ramesh, T. Berg, and E. Learned-Miller. Labeled faces in the wild: A database for studying face recognition in unconstrained environments. Technical report, Technical Report 07-49, University of Massachusetts, Amherst, 2007.
- [78] R. Huang, S. Zhang, T. Li, R. He, et al. Beyond face rotation: Global and local perception gan for photorealistic and identity preserving frontal view synthesis. *arXiv preprint arXiv:1704.04086*, 2017.
- [79] F. N. Iandola, S. Han, M. W. Moskewicz, K. Ashraf, W. J. Dally, and K. Keutzer. Squeezenet: Alexnet-level accuracy with 50x fewer parameters and 0.5 mb model size. *arXiv preprint arXiv:1602.07360*, 2016.
- [80] M. Jaderberg, K. Simonyan, A. Zisserman, et al. Spatial transformer networks. In *NIPS*, pages 2017–2025, 2015.
- [81] R. Jafri and H. R. Arabnia. A survey of face recognition techniques. *Jips*, 5(2):41–68, 2009.
- [82] H. Jegou, M. Douze, and C. Schmid. Product quantization for nearest neighbor search. *IEEE Transactions on Pattern Analysis & Machine Intelligence*, 33(1):117, 2011.
- [83] Y. X. L. X. J. L.-F. Z. Jian Zhao, Yu Cheng. Towards pose invariant face recognition in the wild. In *CVPR*, pages 2207–2216, 2018.

- [84] A. Jourabloo, Y. Liu, and X. Liu. Face de-spoofing: Anti-spoofing via noise modeling. In *The European Conference on Computer Vision (ECCV)*, September 2018.
- [85] M. Kan, S. Shan, H. Chang, and X. Chen. Stacked progressive auto-encoders (spae) for face recognition across poses. In *CVPR*, pages 1883–1890, 2014.
- [86] M. Kan, S. Shan, and X. Chen. Bi-shifting auto-encoder for unsupervised domain adaptation. In *ICCV*, pages 3846–3854, 2015.
- [87] M. Kan, S. Shan, and X. Chen. Multi-view deep network for cross-view classification. In *CVPR*, pages 4847–4855, 2016.
- [88] B.-N. Kang, Y. Kim, and D. Kim. Pairwise relational networks for face recognition. In *The European Conference on Computer Vision (ECCV)*, September 2018.
- [89] I. Kemelmacher-Shlizerman, S. M. Seitz, D. Miller, and E. Brossard. The megaface benchmark: 1 million faces for recognition at scale. In *CVPR*, pages 4873–4882, 2016.
- [90] D. Kim, M. Hernandez, J. Choi, and G. Medioni. Deep 3d face identification. *arXiv preprint arXiv:1703.10714*, 2017.
- [91] M. Kim, S. Kumar, V. Pavlovic, and H. Rowley. Face tracking and recognition with visual constraints in real-world videos. In *CVPR*, pages 1–8. IEEE, 2008.
- [92] T. Kim, M. Cha, H. Kim, J. Lee, and J. Kim. Learning to discover cross-domain relations with generative adversarial networks. *arXiv preprint arXiv:1703.05192*, 2017.
- [93] B. F. Klare, B. Klein, E. Taborsky, A. Blanton, J. Cheney, K. Allen, P. Grother, A. Mah, and A. K. Jain. Pushing the frontiers of unconstrained face detection and recognition: Iarpa janus benchmark a. In *CVPR*, pages 1931–1939, 2015.
- [94] A. Krizhevsky, I. Sutskever, and G. E. Hinton. Imagenet classification with deep convolutional neural networks. In *NIPS*, pages 1097–1105, 2012.
- [95] Z. Lei, M. Pietikainen, and S. Z. Li. Learning discriminant face descriptor. *IEEE Trans. Pattern Anal. Machine Intell.*, 36(2):289–302, 2014.
- [96] J. Lezama, Q. Qiu, and G. Sapiro. Not afraid of the dark: Nir-vis face recognition via cross-spectral hallucination and low-rank embedding. In *CVPR*, pages 6807–6816. IEEE, 2017.
- [97] L. Li, X. Feng, Z. Boukhenafet, Z. Xia, M. Li, and A. Hadid. An original face anti-spoofing approach using partial convolutional neural network. In *IPTA*, pages 1–6. IEEE, 2016.
- [98] S. Z. Li, D. Yi, Z. Lei, and S. Liao. The casia nir-vis 2.0 face database. In *CVPR workshops*, pages 348–353. IEEE, 2013.
- [99] S. Z. Li, L. Zhen, and A. Meng. The hfb face database for heterogeneous face biometrics research. In *CVPR Workshops*, pages 1–8, 2009.
- [100] Y. Li, L. Song, X. Wu, R. He, and T. Tan. Anti-makeup: Learning a bi-level adversarial network for makeup-invariant face verification. *arXiv preprint arXiv:1709.03654*, 2017.
- [101] Y. Li, G. Wang, L. Nie, Q. Wang, and W. Tan. Distance metric optimization driven convolutional neural network for age invariant face recognition. *Pattern Recognition*, 75:51–62, 2018.
- [102] L. Lin, G. Wang, W. Zuo, X. Feng, and L. Zhang. Cross-domain visual matching via generalized similarity measure and feature learning. *IEEE Transactions on Pattern Analysis & Machine Intelligence*, 39(6):1089–1102, 2016.
- [103] T.-Y. Lin, A. RoyChowdhury, and S. Maji. Bilinear cnn models for fine-grained visual recognition. In *ICCV*, pages 1449–1457, 2015.
- [104] C. Liu and H. Wechsler. Gabor feature based classification using the enhanced fisher linear discriminant model for face recognition. *Image processing, IEEE Transactions on*, 11(4):467–476, 2002.
- [105] J. Liu, Y. Deng, T. Bai, Z. Wei, and C. Huang. Targeting ultimate accuracy: Face recognition via deep embedding. *arXiv preprint arXiv:1506.07310*, 2015.
- [106] W. Liu, Y. Wen, Z. Yu, M. Li, B. Raj, and L. Song. SpheroFace: Deep hypersphere embedding for face recognition. In *CVPR*, volume 1, 2017.
- [107] W. Liu, Y. Wen, Z. Yu, and M. Yang. Large-margin softmax loss for convolutional neural networks. In *ICML*, pages 507–516, 2016.
- [108] W. Liu, Y.-M. Zhang, X. Li, Z. Yu, B. Dai, T. Zhao, and L. Song. Deep hyperspherical learning. In *NIPS*, pages 3953–3963, 2017.
- [109] X. Liu, L. Song, X. Wu, and T. Tan. Transferring deep representation for nir-vis heterogeneous face recognition. In *ICB*, pages 1–8. IEEE, 2016.
- [110] X. Liu, B. Vijaya Kumar, C. Yang, Q. Tang, and J. You. Dependency-aware attention control for unconstrained face recognition with image sets. In *The European Conference on Computer Vision (ECCV)*, September 2018.
- [111] Y. Liu, H. Li, and X. Wang. Rethinking feature discrimination and polymerization for large-scale recognition. *arXiv preprint arXiv:1710.00870*, 2017.
- [112] J. Lu, G. Wang, W. Deng, P. Moulin, and J. Zhou. Multi-manifold deep metric learning for image set classification. In *CVPR*, pages 1137–1145, 2015.
- [113] A. M. Martinez. The ar face database. *CVC Technical Report 24*, 1998.
- [114] I. Masi, T. Hassner, A. T. Tran, and G. Medioni. Rapid synthesis of massive face sets for improved face recognition. In *FG 2017*, pages 604–611. IEEE, 2017.
- [115] I. Masi, S. Rawls, G. Medioni, and P. Natarajan. Pose-aware face recognition in the wild. In *CVPR*, pages 4838–4846, 2016.
- [116] I. Masi, A. T. Tr?n, T. Hassner, J. T. Leksut, and G. Medioni. Do we really need to collect millions of faces for effective face recognition? In *ECCV*, pages 579–596. Springer, 2016.
- [117] P. Mittal, M. Vatsa, and R. Singh. Composite sketch recognition via deep network-a transfer learning approach. In *ICB*, pages 251–256. IEEE, 2015.
- [118] B. Moghaddam, W. Wahid, and A. Pentland. Beyond eigenfaces: probabilistic matching for face recognition. *Automatic Face and Gesture Recognition, 1998. Proc. Third IEEE Int. Conf.*, pages 30–35, Apr 1998.
- [119] A. Nech and I. Kemelmacher-Shlizerman. Level playing field for million scale face recognition. In *CVPR*, pages 3406–3415. IEEE, 2017.
- [120] S. J. Pan and Q. Yang. A survey on transfer learning. *IEEE Transactions on knowledge and data engineering*, 22(10):1345–1359, 2010.
- [121] M. Parchami, S. Bashbaghi, E. Granger, and S. Sayed. Using deep autoencoders to learn robust domain-invariant representations for still-to-video face recognition. In *AVSS*, pages 1–6. IEEE, 2017.
- [122] C. J. Parde, C. Castillo, M. Q. Hill, Y. I. Colon, S. Sankaranarayanan, J.-C. Chen, and A. J. O’Toole. Deep convolutional neural network features and the original image. *arXiv preprint arXiv:1611.01751*, 2016.
- [123] O. M. Parkhi, A. Vedaldi, A. Zisserman, et al. Deep face recognition. In *BMVC*, volume 1, page 6, 2015.
- [124] K. Patel, H. Han, and A. K. Jain. Cross-database face antispoofing with robust feature representation. In *Chinese Conference on Biometric Recognition*, pages 611–619. Springer, 2016.
- [125] X. Peng, X. Yu, K. Sohn, D. N. Metaxas, and M. Chandraker. Reconstruction-based disentanglement for pose-invariant face recognition. *intervals*, 20:12, 2017.
- [126] P. J. Phillips, P. J. Flynn, T. Scruggs, K. W. Bowyer, J. Chang, K. Hoffman, J. Marques, J. Min, and W. Worek. Overview of the face recognition grand challenge. In *CVPR*, volume 1, pages 947–954. IEEE, 2005.
- [127] P. J. Phillips, H. Wechsler, J. Huang, and P. J. Rauss. The feret database and evaluation procedure for face-recognition algorithms. *Image & Vision Computing J*, 16(5):295–306, 1998.
- [128] X. Qi and L. Zhang. Face recognition via centralized coordinate learning. *arXiv preprint arXiv:1801.05678*, 2018.
- [129] R. Ranjan, C. D. Castillo, and R. Chellappa. L2-constrained softmax loss for discriminative face verification. *arXiv preprint arXiv:1703.09507*, 2017.
- [130] R. Ranjan, S. Sankaranarayanan, A. Bansal, N. Bodla, J. C. Chen, V. M. Patel, C. D. Castillo, and R. Chellappa. Deep learning for understanding faces: Machines may be just as good, or better, than humans. *IEEE Signal Processing Magazine*, 35(1):66–83, 2018.
- [131] R. Ranjan, S. Sankaranarayanan, C. D. Castillo, and R. Chellappa. An all-in-one convolutional neural network for face analysis. In *FG 2017*, pages 17–24. IEEE, 2017.
- [132] Y. Rao, J. Lin, J. Lu, and J. Zhou. Learning discriminative aggregation network for video-based face recognition. In *CVPR*, pages 3781–3790, 2017.
- [133] Y. Rao, J. Lu, and J. Zhou. Attention-aware deep reinforcement learning for video face recognition. In *CVPR*, pages 3931–3940, 2017.
- [134] C. Reale, N. M. Nasrabadi, H. Kwon, and R. Chellappa. Seeing the forest from the trees: A holistic approach to near-infrared heterogeneous face recognition. In *CVPR Workshops*, pages 320–328. IEEE, 2016.
- [135] K. Ricanek and T. Tesafaye. Morph: A longitudinal image database of normal adult age-progression. In *FG*, pages 341–345. IEEE, 2006.
- [136] E. Richardson, M. Sela, and R. Kimmel. 3d face reconstruction by learning from synthetic data. In *3DV*, pages 460–469. IEEE, 2016.
- [137] E. Richardson, M. Sela, R. Or-El, and R. Kimmel. Learning detailed face reconstruction from a single image. In *CVPR*, pages 5553–5562. IEEE, 2017.
- [138] O. Russakovsky, J. Deng, H. Su, J. Krause, S. Satheesh, S. Ma, Z. Huang, A. Karpathy, A. Khosla, M. Bernstein, et al. Imagenet large scale visual recognition challenge. *International Journal of Computer Vision*, 115(3):211–252, 2015.
- [139] S. Sankaranarayanan, A. Alavi, C. D. Castillo, and R. Chellappa. Triplet probabilistic embedding for face verification and clustering. In

- BTAS, pages 1–8. IEEE, 2016.
- [140] S. Sankaranarayanan, A. Alavi, and R. Chellappa. Triplet similarity embedding for face verification. *arXiv preprint arXiv:1602.03418*, 2016.
- [141] A. Savran, N. Alyüz, H. Dibeklioglu, O. Çeliktutan, B. Gökberk, B. Sankur, and L. Akarun. Bosphorus database for 3d face analysis. In *European Workshop on Biometrics and Identity Management*, pages 47–56. Springer, 2008.
- [142] S. Saxena and J. Verbeek. Heterogeneous face recognition with cnns. In *ECCV*, pages 483–491. Springer, 2016.
- [143] A. Scheenstra, A. Ruifrok, and R. C. Veltkamp. A survey of 3d face recognition methods. In *International Conference on Audio-and Video-based Biometric Person Authentication*, pages 891–899. Springer, 2005.
- [144] F. Schroff, D. Kalenichenko, and J. Philbin. Facenet: A unified embedding for face recognition and clustering. In *CVPR*, pages 815–823, 2015.
- [145] S. Sengupta, J.-C. Chen, C. Castillo, V. M. Patel, R. Chellappa, and D. W. Jacobs. Frontal to profile face verification in the wild. In *WACV*, pages 1–9. IEEE, 2016.
- [146] M. Sharif, S. Bhagavatula, L. Bauer, and M. K. Reiter. Accessorize to a crime: Real and stealthy attacks on state-of-the-art face recognition. In *Proceedings of the 2016 ACM SIGSAC Conference on Computer and Communications Security*, pages 1528–1540. ACM, 2016.
- [147] M. Sharif, S. Bhagavatula, L. Bauer, and M. K. Reiter. Adversarial generative nets: Neural network attacks on state-of-the-art face recognition. *arXiv preprint arXiv:1801.00349*, 2017.
- [148] A. Shrivastava, T. Pfister, O. Tuzel, J. Susskind, W. Wang, and R. Webb. Learning from simulated and unsupervised images through adversarial training. In *CVPR*, volume 3, page 6, 2017.
- [149] K. Simonyan and A. Zisserman. Very deep convolutional networks for large-scale image recognition. *arXiv preprint arXiv:1409.1556*, 2014.
- [150] K. Sohn, S. Liu, G. Zhong, X. Yu, M.-H. Yang, and M. Chandraker. Unsupervised domain adaptation for face recognition in unlabeled videos. *arXiv preprint arXiv:1708.02191*, 2017.
- [151] L. Song, M. Zhang, X. Wu, and R. He. Adversarial discriminative heterogeneous face recognition. *arXiv preprint arXiv:1709.03675*, 2017.
- [152] Y. Sun, Y. Chen, X. Wang, and X. Tang. Deep learning face representation by joint identification-verification. In *NIPS*, pages 1988–1996, 2014.
- [153] Y. Sun, D. Liang, X. Wang, and X. Tang. Deepid3: Face recognition with very deep neural networks. *arXiv preprint arXiv:1502.00873*, 2015.
- [154] Y. Sun, L. Ren, Z. Wei, B. Liu, Y. Zhai, and S. Liu. A weakly supervised method for makeup-invariant face verification. *Pattern Recognition*, 66:153–159, 2017.
- [155] Y. Sun, X. Wang, and X. Tang. Hybrid deep learning for face verification. In *ICCV*, pages 1489–1496. IEEE, 2013.
- [156] Y. Sun, X. Wang, and X. Tang. Deep learning face representation from predicting 10,000 classes. In *CVPR*, pages 1891–1898, 2014.
- [157] Y. Sun, X. Wang, and X. Tang. Sparsifying neural network connections for face recognition. In *CVPR*, pages 4856–4864, 2016.
- [158] C. Szegedy, W. Liu, Y. Jia, P. Sermanet, S. Reed, D. Anguelov, D. Erhan, V. Vanhoucke, A. Rabinovich, et al. Going deeper with convolutions. *Cvpr*, 2015.
- [159] O. Tadmor, Y. Wexler, T. Rosenwein, S. Shalev-Shwartz, and A. Shashua. Learning a metric embedding for face recognition using the multibatch method. *arXiv preprint arXiv:1605.07270*, 2016.
- [160] Y. Taigman, M. Yang, M. Ranzato, and L. Wolf. Deepface: Closing the gap to human-level performance in face verification. In *CVPR*, pages 1701–1708, 2014.
- [161] A. Tewari, M. Zollhöfer, H. Kim, P. Garrido, F. Bernard, P. Perez, and C. Theobalt. Mofa: Model-based deep convolutional face autoencoder for unsupervised monocular reconstruction. In *ICCV*, volume 2, 2017.
- [162] A. T. Tran, T. Hassner, I. Masi, and G. Medioni. Regressing robust and discriminative 3d morphable models with a very deep neural network. In *CVPR*, pages 1493–1502. IEEE, 2017.
- [163] L. Tran, X. Yin, and X. Liu. Disentangled representation learning gan for pose-invariant face recognition. In *CVPR*, volume 3, page 7, 2017.
- [164] M. Turk and A. Pentland. Eigenfaces for recognition. *Journal of cognitive neuroscience*, 3(1):71–86, 1991.
- [165] E. Tzeng, J. Hoffman, K. Saenko, and T. Darrell. Adversarial discriminative domain adaptation. In *CVPR*, volume 1, page 4, 2017.
- [166] C. Wang, X. Lan, and X. Zhang. How to train triplet networks with 100k identities? In *ICCV workshops*, volume 00, pages 1907–1915, 2017.
- [167] D. Wang, C. Otto, and A. K. Jain. Face search at scale: 80 million gallery. *arXiv preprint arXiv:1507.07242*, 2015.
- [168] D. Wang, C. Otto, and A. K. Jain. Face search at scale. *IEEE transactions on pattern analysis and machine intelligence*, 39(6):1122–1136, 2017.
- [169] F. Wang, L. Chen, C. Li, S. Huang, Y. Chen, C. Qian, and C. Change Loy. The devil of face recognition is in the noise. In *The European Conference on Computer Vision (ECCV)*, September 2018.
- [170] F. Wang, W. Liu, H. Liu, and J. Cheng. Additive margin softmax for face verification. *arXiv preprint arXiv:1801.05599*, 2018.
- [171] F. Wang, X. Xiang, J. Cheng, and A. L. Yuille. Normface: l_2 hypersphere embedding for face verification. *arXiv preprint arXiv:1704.06369*, 2017.
- [172] H. Wang, Y. Wang, Z. Zhou, X. Ji, Z. Li, D. Gong, J. Zhou, and W. Liu. Cosface: Large margin cosine loss for deep face recognition. *arXiv preprint arXiv:1801.09414*, 2018.
- [173] L. Wang, V. A. Sindagi, and V. M. Patel. High-quality facial photo-sketch synthesis using multi-adversarial networks. *arXiv preprint arXiv:1710.10182*, 2017.
- [174] M. Wang and W. Deng. Deep visual domain adaptation: A survey. *arXiv preprint arXiv:1802.03601*, 2018.
- [175] W. Wang, Z. Cui, H. Chang, S. Shan, and X. Chen. Deeply coupled auto-encoder networks for cross-view classification. *arXiv preprint arXiv:1402.2031*, 2014.
- [176] X. Wang and X. Tang. Face photo-sketch synthesis and recognition. *IEEE Transactions on Pattern Analysis and Machine Intelligence*, 31(11):1955–1967, 2009.
- [177] X. Wang, Y. Zhou, D. Kong, J. Currey, D. Li, and J. Zhou. Unleash the black magic in age: a multi-task deep neural network approach for cross-age face verification. In *FG 2017*, pages 596–603. IEEE, 2017.
- [178] W. D. Weillong Chai and H. Shen. Cross-generating gan for facial identity preserving. In *FG*, pages 130–134. IEEE, 2018.
- [179] K. Q. Weinberger and L. K. Saul. Distance metric learning for large margin nearest neighbor classification. *Journal of Machine Learning Research*, 10(Feb):207–244, 2009.
- [180] Y. Wen, Z. Li, and Y. Qiao. Latent factor guided convolutional neural networks for age-invariant face recognition. In *CVPR*, pages 4893–4901, 2016.
- [181] Y. Wen, K. Zhang, Z. Li, and Y. Qiao. A discriminative feature learning approach for deep face recognition. In *ECCV*, pages 499–515. Springer, 2016.
- [182] C. Whitelam, K. Allen, J. Cheney, P. Grother, E. Taborsky, A. Blanton, B. Maze, J. Adams, T. Miller, and N. Kalka. Iarpa janus benchmark-b face dataset. In *CVPR Workshops*, pages 592–600, 2017.
- [183] L. Wolf, T. Hassner, and I. Maoz. Face recognition in unconstrained videos with matched background similarity. In *CVPR*, pages 529–534. IEEE, 2011.
- [184] J. Wright, A. Yang, A. Ganesh, S. Sastry, and Y. Ma. Robust Face Recognition via Sparse Representation. *IEEE Trans. Pattern Anal. Machine Intell.*, 31(2):210–227, 2009.
- [185] W.-S. T. WST. Deeply learned face representations are sparse, selective, and robust. *perception*, 31:411–438, 2008.
- [186] W. Wu, M. Kan, X. Liu, Y. Yang, S. Shan, and X. Chen. Recursive spatial transformer (rest) for alignment-free face recognition. In *CVPR*, pages 3772–3780, 2017.
- [187] X. Wu, R. He, and Z. Sun. A lightened cnn for deep face representation. In *CVPR*, volume 4, 2015.
- [188] X. Wu, R. He, Z. Sun, and T. Tan. A light cnn for deep face representation with noisy labels. *arXiv preprint arXiv:1511.02683*, 2015.
- [189] X. Wu, L. Song, R. He, and T. Tan. Coupled deep learning for heterogeneous face recognition. *arXiv preprint arXiv:1704.02450*, 2017.
- [190] Y. Wu, H. Liu, and Y. Fu. Low-shot face recognition with hybrid classifiers. In *CVPR*, pages 1933–1939, 2017.
- [191] Y. Wu, H. Liu, J. Li, and Y. Fu. Deep face recognition with center invariant loss. In *Proceedings of the on Thematic Workshops of ACM Multimedia 2017*, pages 408–414. ACM, 2017.
- [192] S. Xie and Z. Tu. Holistically-nested edge detection. In *ICCV*, pages 1395–1403, 2015.
- [193] E. P. Xing, M. I. Jordan, S. J. Russell, and A. Y. Ng. Distance metric learning with application to clustering with side-information. In *NIPS*, pages 521–528, 2003.
- [194] C. Xiong, X. Zhao, D. Tang, K. Jayashree, S. Yan, and T.-K. Kim. Conditional convolutional neural network for modality-aware face recognition. In *ICCV*, pages 3667–3675. IEEE, 2015.
- [195] L. Xiong, J. Karlekar, J. Zhao, J. Feng, S. Pranata, and S. Shen. A good practice towards top performance of face recognition: Transferred deep feature fusion. *arXiv preprint arXiv:1704.00438*, 2017.
- [196] Y. Xu, Y. Cheng, J. Zhao, Z. Wang, L. Xiong, K. Jayashree, H. Tamura, T. Kagaya, S. Pranata, S. Shen, J. Feng, and J. Xing. High performance large scale face recognition with multi-cognition softmax and feature retrieval. In *ICCV workshops*, volume 00, pages 1898–1906, 2017.
- [197] Y. Xu, S. Shen, J. Feng, J. Xing, Y. Cheng, J. Zhao, Z. Wang, L. Xiong,

- K. Jayashree, and H. Tamura. High performance large scale face recognition with multi-cognition softmax and feature retrieval. In *ICCV Workshop*, pages 1898–1906, 2017.
- [198] Z. Xu, S. Li, and W. Deng. Learning temporal features using lstm-cnn architecture for face anti-spoofing. In *ACPR*, pages 141–145. IEEE, 2015.
- [199] S. Yan, D. Xu, B. Zhang, and H.-J. Zhang. Graph embedding: A general framework for dimensionality reduction. *Computer Vision and Pattern Recognition, IEEE Computer Society Conference on*, 2:830–837, 2005.
- [200] H. Yang, D. Huang, Y. Wang, and A. K. Jain. Learning face age progression: A pyramid architecture of gans. *arXiv preprint arXiv:1711.10352*, 2017.
- [201] H. Yang and I. Patras. Mirror, mirror on the wall, tell me, is the error small? In *CVPR*, pages 4685–4693, 2015.
- [202] J. Yang, Z. Lei, and S. Z. Li. Learn convolutional neural network for face anti-spoofing. *arXiv preprint arXiv:1408.5601*, 2014.
- [203] J. Yang, S. E. Reed, M.-H. Yang, and H. Lee. Weakly-supervised disentangling with recurrent transformations for 3d view synthesis. In *NIPS*, pages 1099–1107, 2015.
- [204] J. Yang, P. Ren, D. Chen, F. Wen, H. Li, and G. Hua. Neural aggregation network for video face recognition. *arXiv preprint arXiv:1603.05474*, 2016.
- [205] M. Yang, X. Wang, G. Zeng, and L. Shen. Joint and collaborative representation with local adaptive convolution feature for face recognition with single sample per person. *Pattern Recognition*, 66(C):117–128, 2016.
- [206] D. Yi, Z. Lei, S. Liao, and S. Z. Li. Learning face representation from scratch. *arXiv preprint arXiv:1411.7923*, 2014.
- [207] Z. Yi, H. Zhang, P. Tan, and M. Gong. Dualgan: Unsupervised dual learning for image-to-image translation. *arXiv preprint*, 2017.
- [208] J. H. Yichen Qian, Weihong Deng. Task specific networks for identity and face variation. In *FG*, pages 271–277. IEEE, 2018.
- [209] J. Yim, H. Jung, B. Yoo, C. Choi, D. Park, and J. Kim. Rotating your face using multi-task deep neural network. In *CVPR*, pages 676–684, 2015.
- [210] L. Yin, X. Wei, Y. Sun, J. Wang, and M. J. Rosato. A 3d facial expression database for facial behavior research. In *FGR*, pages 211–216. IEEE, 2006.
- [211] X. Yin and X. Liu. Multi-task convolutional neural network for pose-invariant face recognition. *TIP*, 2017.
- [212] X. Yin, X. Yu, K. Sohn, X. Liu, and M. Chandraker. Towards large-pose face frontalization in the wild. *arXiv preprint arXiv:1704.06244*, 2017.
- [213] X. Yin, X. Yu, K. Sohn, X. Liu, and M. Chandraker. Feature transfer learning for deep face recognition with long-tail data. *arXiv preprint arXiv:1803.09014*, 2018.
- [214] J. Y. X. W. X. T. Yujun Shen, Ping Luo. Faceid-gan: Learning a symmetry three-player gan for identity-preserving face synthesis. In *CVPR*, pages 416–422. IEEE, 2018.
- [215] E. Zangeneh, M. Rahmati, and Y. Mohsenzadeh. Low resolution face recognition using a two-branch deep convolutional neural network architecture. *arXiv preprint arXiv:1706.06247*, 2017.
- [216] X. Zhan, Z. Liu, J. Yan, D. Lin, and C. Change Loy. Consensus-driven propagation in massive unlabeled data for face recognition. In *The European Conference on Computer Vision (ECCV)*, September 2018.
- [217] T. Y. J. H. Zhanfu An, Weihong Deng. Deep transfer network with 3d morphable models for face recognition. In *FG*, pages 416–422. IEEE, 2018.
- [218] D. Zhang, L. Lin, T. Chen, X. Wu, W. Tan, and E. Izquierdo. Content-adaptive sketch portrait generation by decompositional representation learning. *IEEE Transactions on Image Processing*, 26(1):328–339, 2017.
- [219] J. Zhang, Z. Hou, Z. Wu, Y. Chen, and W. Li. Research of 3d face recognition algorithm based on deep learning stacked denoising autoencoder theory. In *ICCSN*, pages 663–667. IEEE, 2016.
- [220] L. Zhang, L. Lin, X. Wu, S. Ding, and L. Zhang. End-to-end photo-sketch generation via fully convolutional representation learning. In *Proceedings of the 5th ACM on International Conference on Multimedia Retrieval*, pages 627–634. ACM, 2015.
- [221] L. Zhang, M. Yang, and X. Feng. Sparse representation or collaborative representation: Which helps face recognition? In *ICCV*, 2011.
- [222] W. Zhang, S. Shan, W. Gao, X. Chen, and H. Zhang. Local gabor binary pattern histogram sequence (lgbphs): A novel non-statistical model for face representation and recognition. In *ICCV*, volume 1, pages 786–791. IEEE, 2005.
- [223] W. Zhang, X. Wang, and X. Tang. Coupled information-theoretic encoding for face photo-sketch recognition. In *CVPR*, pages 513–520. IEEE, 2011.
- [224] X. Zhang, Z. Fang, Y. Wen, Z. Li, and Y. Qiao. Range loss for deep face recognition with long-tail. *arXiv preprint arXiv:1611.08976*, 2016.
- [225] X. Zhang and Y. Gao. Face recognition across pose: A review. *Pattern Recognition*, 42(11):2876–2896, 2009.
- [226] X. Zhang, X. Zhou, M. Lin, and J. Sun. Shufflenet: An extremely efficient convolutional neural network for mobile devices. *arXiv preprint arXiv:1707.01083*, 2017.
- [227] Y. Zhang, M. Shao, E. K. Wong, and Y. Fu. Random faces guided sparse many-to-one encoder for pose-invariant face recognition. In *ICCV*, pages 2416–2423. IEEE, 2013.
- [228] Z. Zhang, J. Yan, S. Liu, Z. Lei, D. Yi, and S. Z. Li. A face antispoofing database with diverse attacks. In *ICB*, pages 26–31, 2012.
- [229] J. Zhao, J. Han, and L. Shao. Unconstrained face recognition using a set-to-set distance measure on deep learned features. *IEEE Transactions on Circuits and Systems for Video Technology*, 2017.
- [230] J. Zhao, L. Xiong, P. K. Jayashree, J. Li, F. Zhao, Z. Wang, P. S. Pranata, P. S. Shen, S. Yan, and J. Feng. Dual-agent gans for photorealistic and identity preserving profile face synthesis. In *NIPS*, pages 65–75, 2017.
- [231] W. Zhao, R. Chellappa, P. J. Phillips, and A. Rosenfeld. Face recognition: A literature survey. *ACM computing surveys (CSUR)*, 35(4):399–458, 2003.
- [232] T. Zheng and W. Deng. Cross-pose lfw: A database for studying cross-pose face recognition in unconstrained environments. Technical Report 18-01, Beijing University of Posts and Telecommunications, February 2018.
- [233] T. Zheng, W. Deng, and J. Hu. Age estimation guided convolutional neural network for age-invariant face recognition. In *CVPR Workshops*, pages 1–9, 2017.
- [234] T. Zheng, W. Deng, and J. Hu. Cross-age lfw: A database for studying cross-age face recognition in unconstrained environments. *arXiv preprint arXiv:1708.08197*, 2017.
- [235] Y. Zheng, D. K. Pal, and M. Savvides. Ring loss: Convex feature normalization for face recognition. In *CVPR*, June 2018.
- [236] L. Z. Zhengming Ding, Yandong Guo and Y. Fu. One-shot face recognition via generative learning. In *FG*, pages 1–7. IEEE, 2018.
- [237] Y. Zhong, J. Chen, and B. Huang. Toward end-to-end face recognition through alignment learning. *IEEE signal processing letters*, 24(8):1213–1217, 2017.
- [238] E. Zhou, Z. Cao, and J. Sun. Gridface: Face rectification via learning local homography transformations. In *The European Conference on Computer Vision (ECCV)*, September 2018.
- [239] E. Zhou, Z. Cao, and Q. Yin. Naive-deep face recognition: Touching the limit of lfw benchmark or not? *arXiv preprint arXiv:1501.04690*, 2015.
- [240] J.-Y. Zhu, T. Park, P. Isola, and A. A. Efros. Unpaired image-to-image translation using cycle-consistent adversarial networks. *arXiv preprint arXiv:1703.10593*, 2017.
- [241] Z. Zhu, P. Luo, X. Wang, and X. Tang. Deep learning identity-preserving face space. In *ICCV*, pages 113–120. IEEE, 2013.
- [242] Z. Zhu, P. Luo, X. Wang, and X. Tang. Multi-view percepton: a deep model for learning face identity and view representations. In *NIPS*, pages 217–225, 2014.
- [243] Z. Zhu, P. Luo, X. Wang, and X. Tang. Recover canonical-view faces in the wild with deep neural networks. *arXiv preprint arXiv:1404.3543*, 2014.
- [244] W. D. H. S. Zimeng Luo, Jiani Hu. Deep unsupervised domain adaptation for face recognition. In *FG*, pages 453–457. IEEE, 2018.
- [245] T. X. J. K. M.-H. Y. Ziyi Shen, Wei-Sheng Lai. Deep semantic face deblurring. In *CVPR*, pages 8260–8269, 2018.
- [246] W. L. S. G. Zongwei Wang, Xu Tang. Face aging with identity-preserved conditional generative adversarial networks. In *CVPR*, pages 7939–7947, 2018.
- [247] X. Zou, J. Kittler, and K. Messer. Illumination invariant face recognition: A survey. In *BTAS*, pages 1–8. IEEE, 2007.
- [248] S. Zulqarnain Gilani and A. Mian. Learning from millions of 3d scans for large-scale 3d face recognition. *arXiv preprint arXiv:1711.05942*, 2017.